

**OPTIMIZATION OF WIRE ELECTRICAL
DISCHARGE MACHINING OF INCONEL-625
FOR MINIMUM SURFACE ROUGHNESS AND
MAXIMUM MATERIAL REMOVAL RATE**

NSANZUMUHIRE CLAVER

**MASTER OF SCIENCE
(Mechatronic Engineering)**

**JOMO KENYATTA UNIVERSITY OF
AGRICULTURE AND TECHNOLOGY**

**Optimization of Wire Electrical Discharge Machining of
Inconel-625 for Minimum Surface Roughness and Maximum
Material Removal Rate**

Nsanzumuhire Claver

**A thesis Submitted in Partial Fulfillment for the Degree of
Master of Science in Mechatronic Engineering in the Jomo
Kenyatta University of Agriculture and Technology**

DECLARATION

I, Nsanzumuhire Claver do declare that this thesis with title “Optimization of Wire Electrical Discharge Machining of Inconel-625” is my original work and has not been presented in any other University or Institution.

Signature..... Date...../...../.....

Nsanzumuhire Claver

This thesis has been submitted with our approval as University supervisors

Signature..... Date...../...../.....

Prof. Bernard W. Ikua

JKUAT, Kenya

Signature..... Date...../...../.....

Dr. Samuel Karanja Kabini

JKUAT, Kenya

DEDICATION

I dedicate this work to my parents, wife Uwase Diane, friends and supervisors who have been always encouraging me for success.

ACKNOWLEDGEMENT

I thank the Almighty God, who has been on my side at every stage of this work starting from the concept itself. I appreciate him for giving me courage to complete this course. My humble gratitude goes to my supervisors, Prof. B.W. Ikua and Dr. Samuel Karanja Kabini for their willingness to listen to my ideas and for their guidance and advice throughout the course. The Engineering workshops staff deserve special thanks for their willingness to help me carry out my experiments, and in particular, Eng. Daniel Omondi and Mr. Bernard Omego Onyancha who guided me on setting up my experiments. Additionally, I would like to extend my appreciation to my course mate, Denis Mutuma for his encouragement and constructive criticism. I also thank all mechatronic and mechanical engineering members for their criticism to my work during post graduate seminars. Lastly, I thank the Jomo Kenyatta University of Agriculture and Technology for hosting me and make my work successful.

TABLE OF CONTENTS

DECLARATION	ii
DEDICATION	iii
ACKNOWLEDGEMENT	iv
TABLE OF CONTENTS	v
LIST OF TABLES	ix
LIST OF FIGURES	xi
LIST OF APPENDICES	xv
LIST OF ABBREVIATIONS	xv
LIST OF NOTATIONS	xvi
ABSTRACT	xvii
CHAPTER ONE	1
INTRODUCTION	1
1.1 Introduction	1
1.2 Background	1
1.3 Overview of the Properties of Inconel-625	2
1.4 Application of Inconel-625	3
1.5 Machining of Inconel-625	3
1.6 Basic Principle of EDM Process	4
1.7 Problem Statement	5
1.8 Objectives of the Study	6

1.8.1	Main Objective	6
1.8.2	Specific Objectives	6
1.9	Justification of the Research	7
1.10	Scope of the Research	7
1.11	Outline of the Thesis	7
1.12	Summary	8
 CHAPTER TWO		9
 LITERATURE REVIEW		9
2.1	Introduction	9
2.2	Response Surface Methodology	9
2.3	Electrical Discharge Machining	14
2.3.1	Parameters of Electrical Discharge Machining	14
2.3.2	Types of Electrical Discharge Machining	17
2.4	Sinker Electrical Discharge Machining	18
2.5	Wire Electrical Discharge Machining	21
2.5.1	Infuence of Input Parameters on Wire Electrical Discharge Ma- chining Process	22
2.6	Machining of Inconel-625 and Variants Using Wire Electrical Discharge Machining Process	24
2.7	Summary of Gaps	29
2.8	Summary	29

CHAPTER THREE	31
METHODOLOGY	31
3.1 Introduction	31
3.2 Description of Materials Used for Experimentation	31
3.3 Experimental Setup	33
3.3.1 Machining Process Using AWT6S Wire EDM Machine During Preliminary Experimentation	34
3.3.2 Surface Roughness Measurement Using MITUTOYO SJ-30 Sur- face Roughness Tester	36
3.3.3 Measurement of Kerf Width Using PJ311 Profile Projector	38
3.3.4 Calculation of Material Removal Rate	39
3.4 Design of Experiments	40
3.4.1 Determination of Parameter Levels	40
3.4.2 Determination of Number of Experiments	41
3.4.3 Analysis of Variance for Parameter Levels	44
3.5 Optimization of Machining Process Using Taguchi Method	46
3.5.1 Response Tables	49
3.6 Summary	50
CHAPTER FOUR	51
RESULTS AND DISCUSSION	51
4.1 Introduction	51

4.2	Investigation on the influence of input process parameters to machining process	51
4.3	Models for Material Removal Rate and Surface roughness	56
4.3.1	Comparison between predicted and experimental surface roughness and material removal rate	58
4.4	Graphical User Interface	63
4.5	Response Surface Methodology Analysis	65
4.5.1	Surface Contour Plots for Surface Roughness and Material Removal Rate	65
4.5.2	Response Surface Plots for Performance Measures Against Input Parameters	73
4.6	Analysis of Variance Results	76
4.7	Optimization Using Taguchi Method	79
4.8	Validation of Optimal Control Parameters	83
4.9	Summary	84
	CHAPTER FIVE	85
	CONCLUSIONS AND RECOMMENDATIONS	85
5.1	Introduction	85
5.2	Summary	86
	APPENDICES	97

LIST OF TABLES

Table 1.1:	Properties of Inconel-625	2
Table 2.1:	Machining of Inconel-625 using sinker electrical discharge ma- chining	21
Table 2.2:	Influence of control parameters on machining process	24
Table 2.3:	Summary on machining of Inconel-625	28
Table 3.1:	Specifications of equipment used for experimentation	34
Table 3.2:	Parameter-levels used	41
Table 3.3:	Assigned parameter-levels	43
Table 3.4:	Calculation of degrees of freedom	43
Table 4.1:	Response Table for means surface roughness	55
Table 4.2:	Response table for means material removal rate	56
Table 4.3:	Optimal machining conditions	64
Table 4.4:	ANOVA results for Means surafce roughness	76
Table 4.5:	ANOVA results for S/N ratios surface roughness	77
Table 4.6:	ANOVA results for means material removal rate	78
Table 4.7:	ANOVA results for S/N ratios material removal rate	78
Table A.1:	Composition of chemicals in Inconel-625	97
Table B.1:	JSB0601-2001 and ISO standard for surface roughness measure- ment	98

Table C.1: Preliminary results on the effect of pulse-on time on surface roughness and material removal rate	99
Table C.2: Preliminary results on the effect of gap voltage on surface roughness and material removal rate	100
Table C.3: Preliminary results on the effect of wire feed rate on surface roughness and material removal rate	101
Table C.4: Effect of pulse-on time, gap voltage and wire feed rate on surface roughness and material removal rate	101
Table C.5: Effect of pulse-on time, gap voltage and wire feed rate on surface roughness and material removal rate (Continued)	102
Table D.1: The experimental and predicted values for surface roughness and material removal rate	103
Table D.2: Predicted and experimental values for surface roughness and material removal rate (continued)	103

LIST OF FIGURES

Figure 1.1: Wire EDM Erosion process	4
Figure 2.1: Functional set up (a) and Wave form of EDM process (b) . . .	17
Figure 2.2: Schematic diagram of sinker electrical discharge machining . .	18
Figure 2.3: Schematic representation of craters in EDM process	19
Figure 2.4: Schematic representation of wire EDM process	22
Figure 3.1: Specimen used for experimentation	32
Figure 3.2: Photograph of brass cutting wire rolls	32
Figure 3.3: Photograph of de-ionized water tanks	33
Figure 3.4: Equipment used for experimentation	33
Figure 3.5: Set up for cutting process using AWT6S wire EDM machine .	35
Figure 3.6: Schematic block diagram for functional setup of AWT6S wire EDM machine	35
Figure 3.7: Set up for measuring surface roughness using MITUTOYO SJ- 30 surface roughness tester	36
Figure 3.8: Schematic block diagram for setup of MITUTOYO SJ-30 sur- face roughness tester	37
Figure 3.9: Set up for measuring kerf width using PJ311 profile projector	38
Figure 3.10: Schematic block diagram for setup of PJ311 profile projector .	39
Figure 3.11: Photograph of Inconel-625 specimen used in the Study	40
Figure 3.12: Procedure for Taguchi Optimization Process	47

Figure 4.1: Effect of pulse-on time on surface roughness	52
Figure 4.2: Effect of pulse-on time on material removal rate	52
Figure 4.3: Effect of gap voltage on surface roughness	53
Figure 4.4: Effect of gap voltage on material removal rate	53
Figure 4.5: Effect of wire feed rate on surface roughness	54
Figure 4.6: Effect of wire feed rate on material removal rate	55
Figure 4.7: Predicted and experimental surface roughness against pulse-on time	58
Figure 4.8: Predicted and experimental surface roughness against gap voltage	59
Figure 4.9: Predicted and experimental surface roughness against wire feed rate	59
Figure 4.10: Predicted and experimental material removal rate against pulse- on-time	60
Figure 4.11: Predicted and experimental material removal rate against gap voltage	60
Figure 4.12: Predicted and experimental material removal rate against wire feed rate	61
Figure 4.13: Normal plot of the RSM model residuals for surface roughness	62
Figure 4.14: Normal plot of the RSM model residuals for material removal rate	63
Figure 4.15: Screenshot of the user interface and output	64
Figure 4.16: Contour Plot of surface roughness against gap voltage and pulse-on time	66

Figure 4.17: Contour Plot of surface roughness against wire feed rate and pulse-on time	67
Figure 4.18: Contour Plot of surface roughness against wire feed rate and gap voltage	68
Figure 4.19: Contour Plot of material removal rate against wire feed rate and pulse-on time	70
Figure 4.20: Contour Plot of material removal rate against gap voltage and pulse-on time	71
Figure 4.21: Contour Plot of material removal rate against gap voltage and wire feed rate	72
Figure 4.22: Response surface plot for pulse-on time, wire feed rate with surface roughness and material removal rate	73
Figure 4.23: Response surface plot for pulse-on time, gap voltage with surface roughness and material removal rate	74
Figure 4.24: Response surface plot for wire feed rate, gap voltage with surface roughness and material removal rate	75
Figure 4.25: Main effects plot for Means of SR	79
Figure 4.26: Main effects plot for S/N ratios of SR	79
Figure 4.27: Main effects plot for Means of MRR	80
Figure 4.28: Main effects plot for S/N ratios of MRR	81
Figure 4.29: Main effects plot for means of SR and MRR	82
Figure 4.30: Main effects plot S/N ratio of SR and MRR	82
Figure 4.31: Optimized and unoptimized surface roughness	83

LIST OF APPENDICES

Appendix I: Composition of the Specimen Used	97
Appendix II: Surface Roughness Measurement	98
Appendix III: Effect of Input Process Parameters on Machining Output	99
Appendix IV: Predicted and Experimental Output Readings	103
Appendix V: Analysis of Variance Parameters	104
Appendix VI: MATLAB Code for Graphical User Interface	106
Appendix VII: Publications	114

LIST OF ABBREVIATIONS

Adj MS	Adjusted Mean of Squares
Adj SS	Adjusted Sum of Squares
ANOVA	Analysis of Variance
A_{off}	Approach-off time
A_{on}	Approach-on time
CNC	Computer Numerical Control
DF	Degree of Freedom
EDM	Electrical Discharge Machining
F	F-Value for statistical testing
JKUAT	Jomo Kenyatta University of Agriculture and Technology
LDL	Lower Decision Limit
MRR	Material Removal Rate
p	P-Value for significance testing
RSM	Response Surface Methodology
S/N	Signal to Noise Ratio
SeqSS	Sequential Sum of Squares
SR	Surface Roughness
TWR	Tool Wear Rate
UDL	Upper Decision Limit
Wire EDM	Wire Electrical Discharge Machining

LIST OF NOTATIONS

k	Kerf width
n	Number of experiments
t	Machining time
t_{off}	Pulse-off time
t_{on}	Pulse-on time
μs	Microseconds
mm/min	Millimeters per minute
mm³/min	Millimeter cube per minute
y_{ij}	Observed machining experiment response value
V	Volume of metal removed on material during machining
V	Volts
V_g	Gap Voltage
w	Width of cut
f_w	Wire feed rate

ABSTRACT

Inconel-625 is a nickel-alloy based material with properties such as high hardness, oxidation resistance, and high fatigue strength. These properties make it suitable for applications in power generation, marine, and aerospace industries.

Due to high hardness of the material, it is difficult to machine it by conventional machining methods such as turning, milling or grinding. For this reason, Wire Electrical Discharge Machining (Wire EDM) is adopted as an alternative method to machine the material. The competences of this machine includes the fact that it is able to make straight cuts for surface roughness measurement, as opposed to Sinker EDM which is specified in making internal cuts. Once selecting wrong control parameter-levels, the method is accompanied with challenges such as wire breakages, short circuiting of wire, poor surface finish and low material removal rate, leading to high production cost.

In this research, experimental investigations were done to know the influence of pulse-on time (t_{on}), wire feed rate (f_w) and gap voltage (v_g) on surface roughness (SR) and material removal rate (MRR). An Algorithm was developed from mathematical model, developed using Response Surface Methodology (RSM), to correlate input control parameters with output performance measures. The machining process was optimized using Taguchi optimization technique. Inconel-625 plates of 10 mm thickness were used as specimen in experimental work.

It was found out that, for machining of Inconel-625 using wire electrical discharge machining, brass wire as cutting wire, and de-ionized water as medium fluid, the minimum

surface roughness can be achieved for pulse-on time, wire feed rate, and gap voltage of 0.4 μs , 8 mm/min, and 68 V, respectively, whereas for maximum material removal rate, the pulse-on time, wire feed rate and gap voltage should be 0.6 μs , 10 mm/min, and 56 V, respectively. For improved material removal rate and surface roughness, it was observed that the pulse-on time, wire feed rate, and gap voltage could be 0.5 μs , 8 mm/min, and 62 V, respectively. The optimization improved surface roughness and material removal rate by 5.68 % and 3.041 %, respectively.

It is recommended that other output performance measures such as kerf width, corner accuracy and dielectric fluid flow rate may be considered for further investigations.

CHAPTER ONE

INTRODUCTION

1.1 Introduction

This chapter presents a background and overview of Wire Electrical Discharge Machining (Wire EDM) process, overview of the properties of Inconel-625 as well as application and machining of this material. The chapter also discusses the background and motivation behind machining processes. In addition, the problem statement derived from Wire EDM process is presented, and the objectives to tackle the problem are stipulated. Finally, the scope of the study and the thesis outline are given in this chapter.

1.2 Background

Inconel-625 is a nickel alloy based material which is widely used in industrial applications K. G. Kumar, Ramkumar, and Arivazhagan (2015). The properties of this material include resistance to stress cracking, high tensile strength, high corrosion-fatigue resistance, and high hardness. It also has high thermal-fatigue strength, high rupture strength, and oxidation resistance. The outstanding and versatile corrosion resistance under a wide range of pressures and temperatures are the other important properties of Inconel-625. Based on the above mentioned properties, the material is widely used in marine and aerospace Deel (1971). Due to the fact that the material has high hardness, it is difficult to machine using the conventional milling, turning or

grinding operations. Consequently, the material is mainly machined using wire EDM.

1.3 Overview of the Properties of Inconel-625

The chemical composition of Inconel-625 is shown in Appendix A Yangfan, Xizhang, and Chuanchu (2019). The Inconel-625 material has high hardness and strength at high temperature, which make it suitable for the components that require resistance to rupture. The relationship between yield strength, tensile and hardness of the material involves the fact that increased tensile properties for services at moderate temperature are achievable by cold working. However, upon exposure to intermediate temperatures, some hardening occurs in the material which makes it retain its excellent ductility and toughness. Inconel-625 can withstand corrosive environments. In air, fresh water, alkaline, salt water, and neutral salts, almost no attack occurs due to the presence of chromium and nickel that provide resistance to oxidizing environments. In addition, niobium stabilizes the alloy against sensitization during welding whereas pitting and crevice corrosion are prevented by molybdenum. Properties of Inconel-625 are shown in Table 1.1 Yangfan et al. (2019).

Table 1.1: Properties of Inconel-625

Property	Value	Unit
Hardness	256	BHN
Thermal conductivity	64	w/m ^o c
Tensile strength	1103	Mpa
Electrical resistivity	1.26	μ .m
Specific heat	429	J/kg ^o c

With properties of Inconel-625 as shown in Table 1.1, this material is hard to machine using conventional machining processes Němeček, Fiedler, and Fišerová (2015).

1.4 Application of Inconel-625

Due to the constraints of reducing fuel burn, noise generation, and emission of gases, there is high demand for turbomachinery devices. Competitiveness in this demand leads to the need for reducing production cost by controlling the machining speed. In addition, high geometrical accuracy, dimensional accuracy and surface roughness are among major requirements in the area of aeronautical industry. Because of properties of Inconel-625 such as high corrosion resistance, high temperature resistance, the material is widely used in aero engines Deel (1971).

1.5 Machining of Inconel-625

Inconel-625 is an alloy which contains carbides. The hardening effect of this material is caused by the nickel-niobium phase precipitation which transforms to a different form at high temperature. Due to the hardness of of between 248 HV and 253 HV, it is hard to machine this material by means of conventional methods such as turning, milling and grinding Němeček et al. (2015). Difficulties are caused by the high values of temperature and shear forces which are developed during machining process, resulting in quick cutting tool wear. For this reason, wire EDM is among the methods used for machining the material Deel (1971). Wire EDM presents advantages such as, capability of producing complex shapes with high degree of accuracy, absence of mechanical stress during machining as well as ability to machine all electrically conductive metals regardless of their hardness and toughness Carrano, Mehta, and Low (2004); Dewangan (2010); Rajyalakshmi and Ramaiah (2013). However, the process is accompanied with

challenges such as high capital cost, limitation for very large workpiece and formation of heat affected zone (HAZ), recast layer (RCL) and low material removal rate during the machining process Prakash (2008); Sahu (2012); Sethy (2014).

1.6 Basic Principle of EDM Process

The basic principle of wire EDM process is discussed through erosion process as shown in Figure 1.1 Sahu (2012).

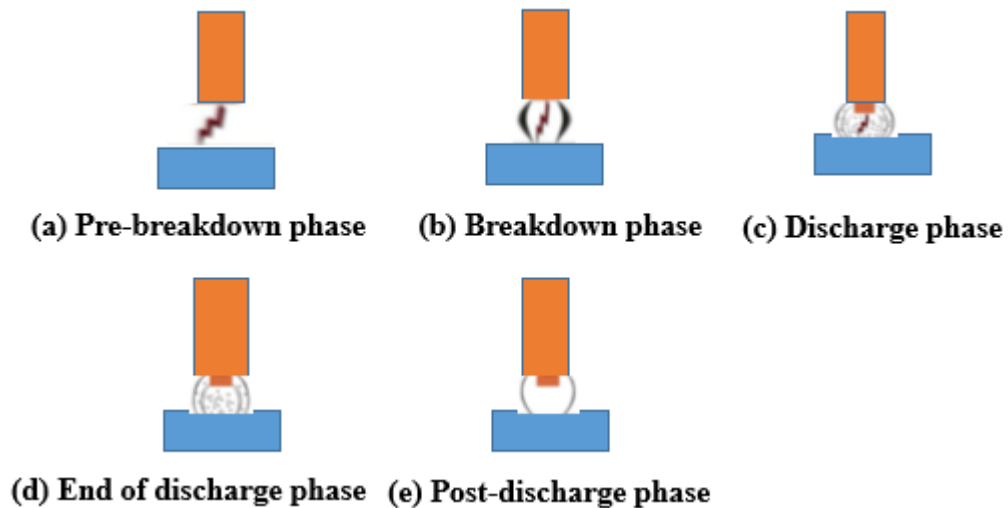


Figure 1.1: Wire EDM Erosion process

Pre-breakdown phase is a phase in which the wire electrode moves towards the workpiece and gap voltage is applied in the machining gap Sethy (2014). *Breakdown phase* is when the applied gap voltage becomes higher than the strength of the dielectric fluid and crosses its boundary limit, causing an electrical breakdown of the fluid. After the electrical breakdown the voltage falls and the current rises, resulting in ionization of the fluid to create a plasma channel in the machining gap. *Discharge phase* is a phase in which the plasma channel grows and the spark discharges are supplied in the machining gap leading to rise in temperature, strong heating of the workpiece and the

cutting wire to melt the workpiece at two electrode surfaces. *End of discharge phase* is a phase in which the plasma channel collapses because the supply of current and voltage is stopped. The last phase in wire electrical discharge machining is the *Post-discharge phase*. At the end of the plasma channel, dielectric fluid plays an important role in cooling process and ha recast layer is deposited in the metal Sahu (2012).

1.7 Problem Statement

Inconel-625 has got a great industrial application. However, due to it's hardness, especially at elevated temperature, it is difficult to machine the material by using conventional processes and therefore, wire EDM is an alternative machining method. In wire EDM, the selection of optimum machining parameters for a specific material presents a challenge. Improper selected parameters may result in lower material removal rate, short-circuiting of wire, wire breakage and poor surface finish Krook, Recina, and Karlsson (2005); Tondy and Tigga (2016). From literature, wire EDM process was optimized with respect to various parameters including discharge current, applied voltage, pulse-off time, wire tension and wire diameter. In wire EDM, the input process parameters with highest influence on material removal rate and surface roughness are pulse-on time, wire feed rate and gap voltage Asgar and Singholi (2018); Babu and Soni (2017); Singh and Singh (2015). Improved machining conditions can be obtained if these parameters are combined for optimization, holding constant all other input process parameters at their optimal levels as reported by previous researchers. In order to eliminate time consuming and costly experiments, an algorithm that uses a mathematical model to correlate surface roughness and material removal rate to var-

ious input variables is needed. As the main contribution of this research to the body of knowledge, the minimum surface roughness and maximum material removal rate is improved since the most influential parameters on these responses are combined for optimization. Finally, with the algorithm developed, optimal machining conditions are obtained with minimum experimentation, thus reduces cost of production.

1.8 Objectives of the Study

1.8.1 Main Objective

The main objective of the research was to optimize the wire EDM process of Inconel-625, through selection of optimum machining parameters for improved surface roughness and material removal rate.

1.8.2 Specific Objectives

In order to accomplish the main objective, the following were the specific objectives:

1. To investigate the influence of pulse-on time, wire feed rate and gap voltage on surface roughness and material removal rate.
2. To develop mathematical model to correlate pulse-on time, wire feed rate and gap voltage with surface roughness and material removal rate and experimentally test the effectiveness of the model.
3. To optimize the process through selection of optimum input parameter-levels of pulse-on time, wire feed rate and gap voltage for minimum surface roughness and maximum material removal rate.

1.9 Justification of the Research

The study was conducted based on industrial applications of Inconel-625 as mentioned in section 1.3, justifying the need for studying its proper machining process, and the fact that it is difficult to machine this material using conventional methods. Undesirable output performance resulting from improper input machining parameter-levels show that there is a need of optimizing the machining process for improved surface roughness and material removal rate. Reduction of experimental cost during machining of Inconel-625 using wire EDM also justifies the need for conducting this study.

1.10 Scope of the Research

This work is limited to investigation of the influence of pulse-on time, wire feed rate and gap voltage on wire EDM of 10 mm thick plates of Inconel-625 and optimization of the process for improved surface roughness and material removal rate. Even though pulse-on time, wire feed rate and gap voltage were the parameters varied, the rest were considered by setting their respective levels at their optimum conditions as reported by previous researchers.

1.11 Outline of the Thesis

This thesis contains five chapters. Chapter one deals with introduction of the research, the existing problem, the objectives and the justification of the research work. Chapter two covers review of the literature on wire EDM process of Inconel-625. Chapter three outlines experimental work done to investigate the effect of input process pa-

rameters on performance measures and optimization process using ANOVA technique. Chapter four covers results and discussion. The conclusions and recommendations are made in chapter five.

1.12 Summary

In this chapter, it is indicated that owing to properties of Inconel-625, the material is used in current technology. However, due to it's hardness, the material is machined by none-conventional processes. In this work, wire electrical discharge machining was adopted for the need of straight cuts needed for surface roughness testing, which could not be possible in the case of sinker electrical discharge machining. The process needs to be optimized for improved machining output in terms of surface roughness and material removal rate, and in order to reduce the need for experiments which are costly and time consuming, an algorithm needs to be developed based on mathematical model that collerates input control parameters with output performance measures.

CHAPTER TWO

LITERATURE REVIEW

2.1 Introduction

This chapter presents an overview on Response Surface Methodology as applied for modelling process , both sinker and wire electrical discharge machining, influence of input process parameters on wire EDM process, machining of Inconel-625 and vaariants using wire EDM, and summary of gaps identified from review of the literature.

2.2 Response Surface Methodology

Response Surface Methodology (RSM) refers to the collection of statistical and mathematical methods used for empirical model building. The method is based on the fitness of polynomial equation to experimental data, that describes the trait of how the output variables relate to the input variables Bezerra, Santelli, Oliveira, Villar, and Escalera (2008); Jensen (2008); Mäkelä (2017). The objective of this method is to optimize a response which is influenced by several independent variables by design of experiments. It is useful for statistical previsions, modeling and analysis of responses affected by many variables. Response surface modeling is built on the approximation of the correct performance of a response. The model response is expressed as Carley, Kamneva, and Reminga (2004):

$$y = f(\theta_1, \theta_2, \theta_3, \dots, \theta_k) + \epsilon \tag{2.1}$$

Where $\theta_1, \theta_2, \theta_3$ and θ_k represent the variables and ϵ represents the residual related to the experiments. The elementary model for Response Surface Methodology, is a linear function expressed as Alexandrov and Lewis (2001):

$$y_i = \beta_0 + \sum_{i=1}^k \beta_i x_i + \epsilon \quad (2.2)$$

Where k represents the number of variables, β_0 represents the average value of y_i , β_i represents the first order coefficients, and x_i constitute the coded factors of the variables. If the responses of the model present a curvature, a second-order model is used to describe the interaction between different variables, which is expressed as Joshi, Sherali, and Tew (1998):

$$y_i = \beta_0 + \sum_{i=1}^k \beta_i x_i + \sum_{1 \leq i \leq j}^k \beta_{ij} x_i x_j + \epsilon \quad (2.3)$$

Where β_{ij} constitute the interaction coefficients. However, to determine a critical point, the polynomial function must contain quadratic terms as Sanders, Sarh, and Gökulp (1997):

$$y_i = \beta_0 + \sum_{i=1}^k \beta_i x_i + \sum_{i=1}^k \beta_{ii}^2 x_i^2 + \sum_{1 \leq i \leq j}^k \beta_{ij} x_i x_j + \epsilon \quad (2.4)$$

Where β_{ii} represents the second-order coefficients.

The assessment of the fitted model is authentically done by the application of analysis of variance (ANOVA). Analysis of variance compares the variation expressed by the model with the variation of model residuals, thus evaluating the significance of the regression model used for predictions in comparison to the real data. The assessment

of the data variation is done by studying the corresponding dispersion. The evaluation of the square deviation d_i^2 that each observation (y_i) or corresponding replicates (y_{ij}) present in relation to the average (\bar{y}) is presented as Nourbakhsh, Rajurkar, Malshe, and Cao (2013):

$$d_i^2 = (y_{ij} - \bar{y})^2 \quad (2.5)$$

Total sum of the square (SS_{tot}) is the sum of all square observed in association to the data set, and is presented as Devarasiddappa, George, Chandrasekaran, and Teyi (2016):

$$SS_{tot} = \sum_{i=1}^n (y_i - \bar{y})^2 = SS_{reg} + SS_{res} \quad (2.6)$$

Where (SS_{reg}) represents the sum of squares due to regression and (SS_{res}) stands for the sum of squares due to the residuals. The sum of all squares due to residuals can be subdivided into sum of the square due to pure error (SS_{pe}) and sum of the square due the lack of fit (SS_{lof}) as Velleman and Welsch (1981):

$$SS_{res} = \sum_{i=1}^n (y_i - \hat{y})^2 = SS_{pe} + SS_{lof} \quad (2.7)$$

The model sum of squares is equal to the sum of the square (SS_{tot}) plus the generated residuals by the model (SS_{res}) as Griffith (1989):

$$SS_{mod} = SS_{tot} + SS_{res} \quad (2.8)$$

The pure error is given by Arminian, Kang, Kozak, Houshmand, and Mathews (2008):

$$SS_{pe} = \sum_{i=1}^m \sum_{j=1}^{nr} (y_{ij} - \bar{y}_i)^2 \quad (2.9)$$

Where SS_{pe} is the estimate of a pure error, nr is the number of replicas at a design location and m is the number of design locations where replicas were performed. The sum of the square due the lack of fit (SS_{lof}) can be obtained as Wang and Conerly (2003):

$$SS_{lof} = SS_{res} - SS_{pe} \quad (2.10)$$

Fishers distribution is used to compare the variation of the regression media squares and the variation of the residuals media squares while considering the degrees of freedom (DOF) associated to these squares as Bower (2000):

$$\frac{MS_{reg}}{MS_{res}} \approx FV_{reg}, V_{res} \quad (2.11)$$

Where the square media of regression is represented as (MS_{reg}), the squares media of residuals as (MS_{res}), the DOF related to the regression as (V_{reg}) and the DOF related to residuals as (V_{res}). If the F test presents a value greater than the F value tabulated, the experimental data is well fitted with the regression model where the model is viewed as statistically important. The lack of fit test is also used as an alternative for evaluating the signigance of the regression model where it is expected that it becomes insignificant, because it is desirable to fit the data. The lack of fit test

is described as Helsel (2011):

$$\frac{MS_{tot}}{MS_{pe}} \approx FV_{tof}, V_{pe} \quad (2.12)$$

Where, MS_{tof} represents the systems lack of fit random errors, MS_{pe} represents the pure errors. The DOF related to lack of fit and pure error are represent as V_{tof} and V_{pe} , respectively. A higher lack of fit means that the regression model must be improved. In summary, a well fitted model must present a non significant lack of fit and a significant regression. The model quality is described by the coefficient of determination, which determines the percentage of the original data explained by the model, and described as Cramer (2002):

$$R^2 = \frac{SS_{mod}}{SS_{tot}} = 1 - \frac{SS_{res}}{SS_{tot}} \quad (2.13)$$

Where R^2 is the coefficient of determination. It's weakness is that it continues increasing as there is addition of more terms to the model thus resulting to over-fitting. To solve the R^2 problem of over-fitting, it is introduced the adjusted R-squared, which is calculated as Cramer (2002):

$$R_{adj}^2 = 1 - \left(\frac{SS_{res}}{n-p} \times \frac{n-1}{SS_{tot}} \right) \quad (2.14)$$

This covers the degrees of freedom in the model, by decreasing in value if the model terms increase.

2.3 Electrical Discharge Machining

Electrical discharge machining refers to a method used to machine electrically conducting metals or metals that are hard to machine using the traditional techniques. In EDM, the input parameters are responsible of controlling the machining process. For example, the applied voltage causes discharge across the spark gap which removes material by a thermal process. The spark energy is controlled so as to melt and vaporize the material from the workpiece. Flushing process is applied to remove machined particles. Bisaria and Shandilya (2015); Pham, Dimov, Bigot, Ivanov, and Popov (2004).

2.3.1 Parameters of Electrical Discharge Machining

The parameters of electrical discharge machining are classified in two main categories that are process and response parameters. The process parameters are the independent input variables such as spark gap, duty cycle, pulse-on time and pulse-off time. The response parameters are the dependent variables which include the material removal rate, surface roughness, tool wear rate, recast layer, heat affected zone, taper and overcut.

Pulse-on time (t_{on}) is referred to as the period during which there is flow of current in the gap between electrode and workpiece. During this period, the amount of energy used is directly proportional to the metal removal Kansal, Singh, and Kumar (2005). The electrical discharge machining process erosion takes place in the form of melting and vaporization of both the tool and work material at the same time. Thus under a longer pulse duration there will be more material melting and vaporizing. Compared to

a shorter pulse-on time, the crater produced is be broader. However, some of past experimental research work has reported that there should be an optimal pulse duration yielding high performance measures Mohan, Rajadurai, and Satyanarayana (2004).

Pulse-off time (t_{off}) is referred to as the waiting period between two pulses. This is the period where there is no machining thus allowing melting of the material to vaporize. This parameter affects the the speed of cutting process and it's stability. Shorter pulse-off time gives high material removal rate and causes more sparks to be unstable in the machining zone. With a very short pulse interval, there is high arcing probability caused by the inability of the dielectric to recover it's strengthKansal, Singh, and Kumar (2007); Saha and Choudhury (2009).

Spark gap is referred to as the distance between the workpiece and the electrode during the machining process. There should be a suitable gap maintained in order to achieve the gap stability and good performanceCrookall and Heuvelman (1971).

Duty cycle is referred to as the percentage pulse-on time relative to total cycle time. Duty cycle helps to indicate the degree of operation based on efficiency. Increase in duty cycle causes the intensity of sparks to increase thus leading to a higher cutting speed. The duty cycle (DC) is calculated as Lee and Li (2001):

$$DC = \frac{t_{on}}{t_{on} + t_{off}} \quad (2.15)$$

Polarity is referred to when the connection of the tool electrode and workpiece are either positive or negative terminals. Polarity can affect the stability or the speed of the machining process. When there is generation of electrical discharge, the electrons

get dispatched from the negative polarity. They then collide with neutral molecules between the electrode and the workpiece causing the ionization process. Ionization occurs when the electrons flow to the positive surface terminal Chow, Yan, and Huang (1999). In this work, negative polarity was used, this means that the cutting wire connected was connected as negative and the workpiece as positive.

Material removal rate (MRR) is the rate of metal erosion from the workpiece. It helps to indicate cost effectiveness and efficiency of the machining process Maher, Sarhan, and Hamdi (2015). During electrical discharge machining, there is an electric field formed in the gap. The formation of the electric field depends on the distance between the workpiece and tool electrode. There is emission of electrons once the potential difference between electrodes is high. The emitted electrons accelerate towards the workpiece via the dielectric medium. With time, the electrons gain velocity causing collisions between them and the dielectric molecules which result to ionization of the dielectric molecules Amorim and Weingaertner (2002). These collisions enhance generation of more positive ions caused by the acceleration of electrons.

The process results into a pool of ions and electrons in the dielectric medium which is in the spark gap. The concentration turns high, causing the formation of the plasma. Such a plasma has a very small electrical resistance and therefore there is a large number of ions from the workpiece to the tool and electrons flow from the tool to the workpiece. The electrical energy in this process is referred to as the thermal energy of the spark Rajurkar, Zhu, McGeough, Kozak, and De Silva (1999). The kinetic energy of the electrons and ions is converted into the thermal energy. This enables consequent material removal and causes melting. Functional setup and wave form of the EDM

process is shown in Figure 2.1.

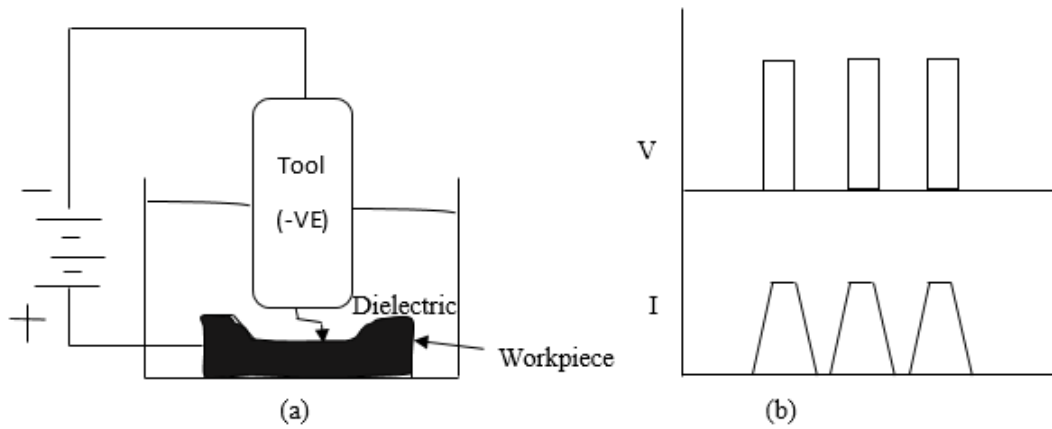


Figure 2.1: Functional set up (a) and Wave form of EDM process (b)

The potential difference is withdrawn during the intervals as shown in Figure 2.1 (b), the plasma channel is not sustained anymore causing it's collapse as it generates pressure or shock waves. This leads to evacuation of the molten material that forms a crater of removed material around the site of the spark Thidé (2004).

2.3.2 Types of Electrical Discharge Machining

There are two types of EDM, i.e., wire EDM and sinker EDM. For both types, the setup of the equipment is composed of two electrodes. For wire EDM, the tool is a thin wire made of copper or brass while for sinker EDM, the electrode is a graphite, copper or tungsten carbide material Rao, Satyanarayana, and Praveen (2008). The main difference between wire EDM and sinker EDM is the type of electrode used. A wire EDM uses thin conductive wire to electrically discharge power and erode a path on a workpiece, while a sinker EDM uses shaped or sized electrodes to erode a workpiece. The sinker EDM has two metal parts submerged together in a dielectric medium Pham et al. (2004).

2.4 Sinker Electrical Discharge Machining

Schematic diagram of sinker electrical discharge machining is shown in Figure 2.2.

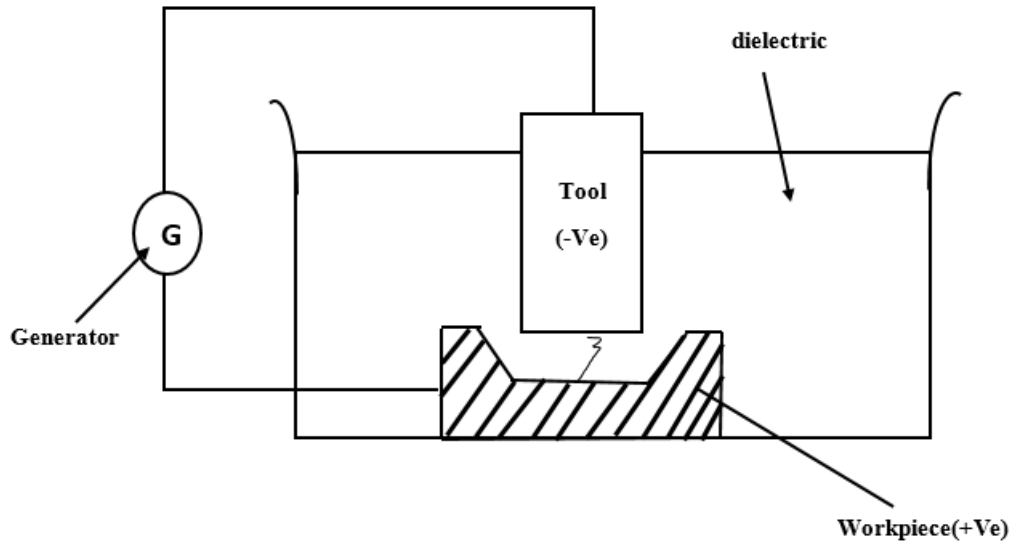


Figure 2.2: Schematic diagram of sinker electrical discharge machining

In sinker EDM as shown in Figure 2.2, the potential difference is realized between the tool and workpiece all immersed in a dielectric medium. Based on the potential difference applied and the distance between the tool and the workpiece, there will be formation of an electric field thus subjecting the tool free electrons into electrostatic forces. When the electrons' bonding energy becomes less, there is emission of the latter from the tool. The emitted electrons are cold and they accelerate to the job via the dielectric medium. After the electrons gain velocity and energy, they are able to accelerate towards the job thus forming collision with dielectric molecules. Such collisions lead to ionization of the dielectric molecules depending on the amount of ionization energy of the dielectric molecule and the electron. Due to collisions there are more positive electrons and ions generated. This process is cycle that keeps on

repeating itself thus increasing the concentration of ions and electrons at the spark gap. High concentration trigger a large number of electrons move from the tool to the job while the ions move from the job to the tool. The electrical energy is termed as thermal energy of the spark. However, the high-speed ions impinge on the tool and electrons on the job. The kinetic energy of the electrons and ions on impact with the surface of the job and tool respectively is converted into thermal energy or heat flux. Such intense localized heat flux leads to extreme instantaneous rise in temperature leading to removal of the material. Instant melting and vaporization causes material removal. The removal of the molten metal is done partially. Withdraw of the potential difference leads to no sustainability of the plasma channel. Collapse of the plasma channel triggers generation of shock waves or pressure and evacuation of the molten material that forms a crater Banker, Parmar, and Parekh (2013).

The hemisphere’s mathematical model represents the molten crater dimensions thus explaining the amount of energy applied in erosion of a crater per spark. A schematic representation of craters in EDM process is shown in Figure 2.3 Popa, Contiu, and Pop (1866).

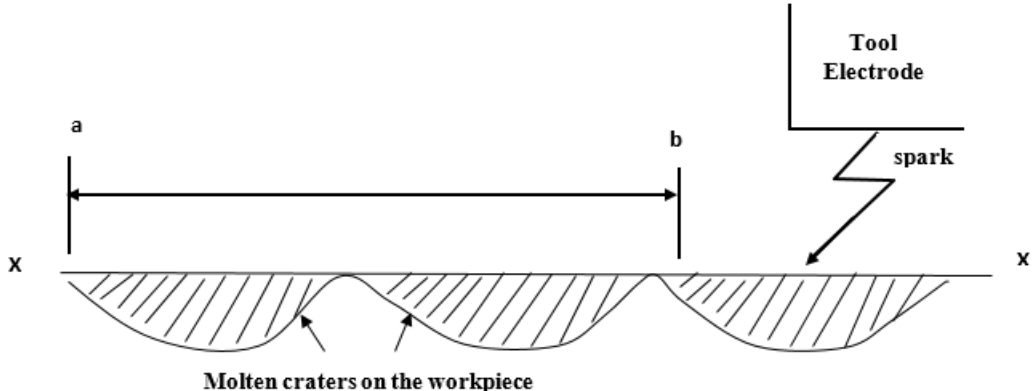


Figure 2.3: Schematic representation of craters in EDM process

In assumption, the Material removed (Mr) in a single spark will be proportional directly to the spark energy (Ei), given by Joshi et al. (1998):

$$E_i = V_p I_p t_{on} \quad (2.16)$$

Hence,

$$M_r = \alpha V_p I_p t_{on} \quad (2.17)$$

Where V_p is the voltage of a one pulse, I_p is the current of a one pulse, t_{on} is the pulse-on time, t_{off} is the pulse-off time, and α represents a constant of the removal of material. Hence, the *workpiece MRR* is presented by material removed in a unit time as Rajmohan, Prabhu, Rao, and Palanikumar (2012):

$$MRR = \alpha V_p I_p t_{on} \frac{1}{t_{on} + t_{off}} \quad (2.18)$$

Electrode wear ratio is referred to as the ratio of electrode's wear weight to that of the workpiece, obtained as K. Kumar, Sivasubramanian, and Kalaiselvan (2009):

$$EWR = \left(\frac{W_e}{W_w} \right) 100 \quad (2.19)$$

Where W_e represents wear weight of the electrode and W_w represents wear weight of workpiece.

The roughness of the surface helps to measure the finely spaced surface irregularities about the machined workpiece's surface and it is measured by various types of surface

roughness testers. The typical discharge energy per spark in wire EDM is 40 micro-joules Giridharan and Samuel (2016). Some of research works done on machining of Inconel-625 using sinker Eletrical discharge machining are shown in Table 2.1.

Table 2.1: Machining of Inconel-625 using sinker electrical discharge machining

Parameter	Technique	Findings	Author
$t_{on}, t_{off}, I_P, P_f$ TWR, MRR	Composite desirability	higher t_{on} and I_P , higher MRR The higher P_f , higher MRR	Ansari and Bansal (2017)
t_{on}, t_{off}, I_P TWR, MRR	Taguchi	MRR, I_P then t_{on} TWR, t_{on} then t_{off}	Vates, Singh, and Singh (2016)
$t_{on}, t_{off}, I_P, P_f$ TWR, MRR	Taguchi	higher t_{on} and P_f , higher MRR The higher t_{off} , lower MRR	Pramanik and Basak (2019)

2.5 Wire Electrical Discharge Machining

Wire EDM is referred to as a unique form of the electrical discharge process where a continuous moving thin wire is used as one electrode. The workpiece material is melted and evaporated to help achieve the material removal mechanism. The melting and evaporation processes are done at every electrical discharge spot. The debris are ejected and later flushed away by the dielectric fluid. Wire EDM effectuates a plasma channel in-between the anode and cathode by using electrical energy which is converted into thermal energy, capable of producing temperatures between 8000-12,000 °C Maher et al. (2015). Material erosion begins from the workpiece and there is a wire separated by a stream of dielectric fluid and guided by a diamond or sapphire guide. The schematic representation of wire EDM process is shown in Figure 2.4 Pham et al. (2004).

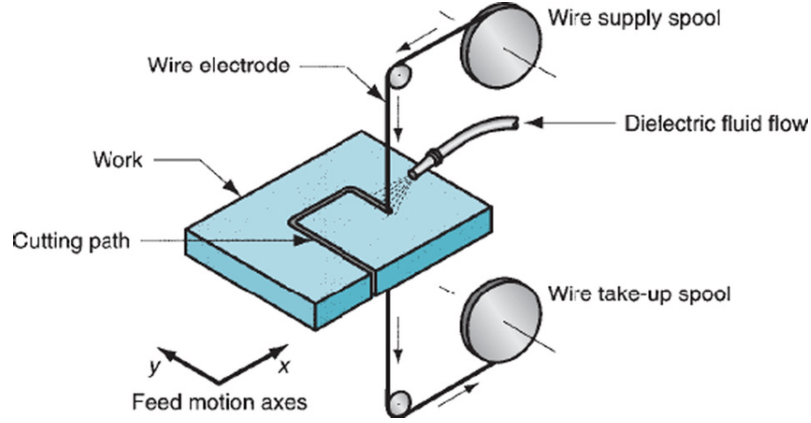


Figure 2.4: Schematic representation of wire EDM process

In wire EDM process, the MRR is calculated as:

$$MRR = \frac{lwk}{t} \quad (2.20)$$

Where l represents length of cut, w represents the width of cut, k represents kerf and t is the machining time.

2.5.1 Influence of Input Parameters on Wire Electrical Discharge Machining Process

The pulse-on time is a parameter that designates peak discharge current and pulse width during machining process. The higher the value is set, the higher the resulting peak discharge current and pulse width. As a result, the cutting speed increases and causes tendency of cutting wire breakage and increase in surface roughness during pulse discharge. On the other hand, the pulse-off time (t_{off}) designates the discharge stop time, which is the period between two consecutive discharge pulses. The higher the value is set, the averaged energy during discharge becomes lower, the cutting speed

reduces, and the cutting wire does not easily break during pulse discharge.

The approach-on time (A_{on}) designates discharge pulse time during carbon accumulation. This phenomena occurs when the material is heated enough and the oxygen starts producing carbon dioxide. This parameter means the same as the pulse-on time but the starting time is different. The lower the value is set, the slower the resulting cutting speed and cutting wire does not easily break during coarse discharge. In opposition to the approach-on time, for the approach-off time (A_{off}), the higher the value at which this parameter is set, the slower cutting speed during pulse discharge and cutting wire does not easily break. Wire tension (t_w) is a parameter which adjusts the magnitude of tension in the cutting wire. The larger value means the larger wire tension with higher straightness and faster discharge speed. If wire tension is too high, there is a tendency of wire breakage during coarse discharge. The wire feed rate (f_w) is a parameter which adjusts the feed rate of the cutting wire. The higher value of this parameter means the faster feed of the cutting wire, which reduces the likelihood of occurrence of cutting wire breakage and enhances cutting precision. The water pressure is a parameter that chooses the magnitude of pressure of dielectric fluid during discharge. The higher value, the higher pressure and more residues are ejected during coarse discharge and the discharge energy is enhanced to increase the cutting speed.

Another parameter of wire electrical discharge machining is the gap voltage (v_g). This parameter, with the help of pulse-on time, decides the discharge speed and gap groove. The smaller value means the faster discharge speed and the smaller gap groove and vice versa. Once the value is set too small, the discharge becomes unstable and the cutting wire breaks easily during coarse discharge Abbas, Solomon, and Bahari (2007);

Maier et al. (2015); Muthuramalingam and Mohan (2015). Summary of influence of control parameters on machining process is shown in Table 2.2.

Table 2.2: Influence of control parameters on machining process

Item	Level	Influence	Reference
t_{on}	High	Longer discharge time	Vates et al. (2016)
		Poor surface finish	
		Wider kerf width	
		Higher MRR	
		Higher stability	
t_{off}	High	More flushing time	Vates et al. (2016)
		Smother surface finish	
		Lower MRR	
		Fewer micro-cracks	
		Wider spark gap	
V_g	High	Lower MRR	Vates et al. (2016)
		Poor SR	
		Stable discharge	
f_w	High	Higher MRR	Alias, Abdullah, and Abbas (2012)
		Higher SR	
		Frequent wire breakage	
t_w	High	Stiffer wire	Sanghani and Acharya (2016)
		Wire breakage	
		Poor surface finish	
P_f	High	Faster flushing	Pramanik and Basak (2019)
		Smoother surface finish	
		Fewer short circuits	

2.6 Machining of Inconel-625 and Variants Using Wire Electrical Discharge Machining Process

There has been a great deal of interest in optimization of wire electrical discharge machining process for Inconel-625 and a number of such studies have been reported in the literature. For instance, Abbas and Solomon (2013), conducted a study on the influence of pulse-on time, pulse-off time and peak current in the wire electrical discharge machining of Inconel-625 by applying Taguchi orthogonal array to optimize

these parameters for minimization of the roughness of the surface. In that study, the surface roughness was found to increase as the pulse-on time increases and decrease as the pulse-off time (t_{off}) decreases, whereas the peak current was found to have no significant effect on the process.

Tonday and Tigga (2016), investigated on the influence of cutting process parameters on material removal rate and surface roughness in wire electrical discharge machining of Inconel-625. The input parameters were pulse-on time, pulse-off time, wire tension, and peak current. In the study, the researcher used Taguchi technique and analysis of variance to analyze the influence of these parameters on output performance measures. As results, it was concluded that wire tension had no much effect on both surface roughness and material removal rate. The pulse-on time was found to have much influence on the two output parameters, whereas pulse-off time influences less on surface roughness than on material removal rate. It was also found that the peak current has the largest influence on the surface roughness.

Shah, Mevada, and Khatri (2013), investigated on metal removal rate and surface characteristics of Inconel-600 using electrical discharge machining. In the study, the input parameters were peak current, pulse-on time and pulse-off time. It was concluded that the increase in peak current and pulse-on time improves cutting speed and surface roughness whereas the increase in pulse-off time decreases the cutting speed. However, the researcher did not investigate on gap voltage which may affect the cutting.

Abhishek, Datta, Biswal, Mahapatra, et al. (2017), studied on optimization of machining performance in electro-discharge machining of Inconel-625. In the research, application of fuzzy inference systems in conjugation with Taguchi philosophy has been

demonstrated as an efficient route for simultaneous optimization of multi-requirements of process performance on material removal rate, tool wear rate, and surface roughness. The input parameters considered were the pulse-on time, peak current, flushing pressure and gap voltage. The optimum levels of these parameters were found to be 200 μ s, 5 A, 0.6 bar, and 90 V, respectively.

Datta, Biswal, Mahapatra, et al. (2019), investigated on the machining performance of wire electrical discharge machining of Inconel-625 and Taguchi technique was used to optimize the process. The input parameters which included gap voltage, peak current, pulse-on time, duty factor and flushing pressure, were found to have effects on the process and on output performance measures. Karsh and Singh (2018), conducted a study on the influence of pulse-off time and peak current on surface roughness and cutting speed in Wire EDM of Inconel-625. In the study, Taguchi orthogonal array was used for experimental work. The research revealed that surface roughness decreases with the increase in pulse-off time whereas the cutting speed increases with the increase in peak current. However, this study did not consider the effect of pulse-on time on the machining process.

Hewidy, El-Taweel, and El-Safty (2005), investigated on wire electrical discharge machining of Inconel-601. In the study, peak current, pulse on time, wire tension and water pressure were considered as input parameters whereas metal removal rate, wear ratio and surface roughness were the output process output parameters. The researchers did modeling of the process using response surface methodology (RSM) and found out that there is an increase in volumetric metal removal rate due to the increase in pulse-on time.

Newton, Melkote, Watkins, Trejo, and Reister (2009), conducted an experimental work on recast layer formation in Wire EDM of Inconel-718. In their study, the average thickness of recast layer was found to increase with the increase in pulse duration and peak discharge current. Because the recast layer formation is proportional to the material removed, then the cutting speed can also be determined by the pulse-on time. Since Inconel-601 and Inconel-718 are both grades of Inconel-625, the materials have similar properties such as hardness and resistance to elevated temperature. Consequently, there is a probability that the pulse-on time might also have a significant influence in machining of Inconel-625, and yet this parameter was not considered in the study.

Va, Ab, Rc, and Md (2010), studied on Wire EDM of Incoloy 800 using Grey Relational Analysis, Taguchi method and analysis of variance. The cutting conditions for optimal cutting speed, surface roughness and kerf was investigated considering, pulse-on time, gap voltage, pulse off-time and wire feed rate as input variables. The study revealed that all these input parameters have considerable influence on machining performance. Both Incoloy-800 and Inconel-625 have some similar properties such as corrosion resistance, heat resistance, resistance to stress, corrosion resistance, resistance to cracking at elevated temperatures, as well as rupture and creep strength, K. G. Kumar et al. (2015). Therefore, the gap voltage, pulse-on time and wire feed rate revealed to have affected the machining performance in Wire EDM of Incoloy 800 can also be investigated for Inconel-625.

Rajyalakshmi and Ramaiah (2013), investigated on cutting speed and surface roughness in Wire EDM of Inconel-825. In the study, orthogonal array design of experiment was combined with grey relational analysis to find the optimum cutting conditions.

It was observed that the pulse-on time, pulse-off time, gap voltage, flushing pressure, wire feed rate, wire tension should be set to optimal values for improved cutting speed and surface roughness .

Sharma, Chakradhar, and Narendranath (2015) conducted a study on cutting speed, surface roughness, recast layer (RLT), topography and micro hardness of Inconel-706 for turbine disk application. The RLT and micro hardness have been examined using the low and high settings of pulse-on time and gap voltage. Energy dispersive analysis of X-rays has been carried out to study the metallurgical changes in the machined surface. The study revealed that pulse-off time, pulse-on time, and gap voltage are most important factors. It was also found out that for improved cutting speed and surface roughness, the wire feed and flushing pressure should be 6 mm/min and of 1.96 Pa respectively. Findings from different authors are summarized in Table 2.3.

Table 2.3: Summary on machining of Inconel-625

Parameter	Method	Finding	Reference
t_{on}, t_{off}, I_p	Taguchi	$t_{on} = 13 \mu s$	Abbas and Solomon (2013)
		$t_{off} = 10 \mu s$ $I_p = \text{No effect}$	
$t_{on}, t_{off}, T_w, I_p$	Taguchi	$t_{on} = 6 \mu s$	Tonday and Tigga (2016)
		$t_{off} = 8 \mu s$ $T_w = 15 \text{ N}$ $I_p = 17 \text{ A}$	
I_P, t_{on}, t_{off}	RSM	$t_{on} = 16 \mu s$	Shah et al. (2013)
		$t_{off} = 23 \mu s$ $I_p = 2 \text{ A}$	
t_{on}, I_p, P_f, V_g	Fuzzy	$t_{on} = 200 \mu s$	Abhishek et al. (2017)
		$I_p = 5 \text{ A}, V_g = 90 \text{ V } \mu s$ $P_f = 0.6 \text{ bar}$	
V_g, I_p, t_{on}, P_f	Taguchi	$V_g = 72 \text{ V}, I_p = 3 \text{ A}$	Datta et al. (2019)
		$t_{on} = 92 \mu s$ $P_f = 0.9 \text{ bar } \mu s$	

2.7 Summary of Gaps

From literature, it can be seen that previous researchers tried to optimize the machining process with respect to various input process parameters, but the combination of pulse-on time, wire feed rate and gap voltage was not considered. In wire electrical discharge machining, pulse-on time, wire feed rate and gap voltage are the input parameters with the highest influence on surface roughness and material removal rate Asgar and Singholi (2018); Babu and Soni (2017); Singh and Singh (2015). Improved machining conditions can be obtained if these parameters are combined for optimization, holding constant all other input process parameters at their optimal levels. In this work, wire electrical discharge machining process of Inconel-625 is optimized using Taguchi optimization method. Experiments are carried out to find out the effect of combination of the most influential parameters on surface roughness and material removal rate, and a graphical user interface that uses a mathematical model to correlate these output performance measures to various input variables was developed to reduce the need for experiments which are costly and time consuming.

2.8 Summary

Response surface methodology, as applied in this work for modeling, is discussed in this chapter. Although previous researchers have been trying to optimize the wire electrical discharge machining of Inconel-625 with respect to different process parameters, the optimization can be improved by considering combination of pulse-on time, wire feed rate and gap voltage, parameters that were reported to be the most influential on

surface roughness and material removal rate, regardless of the material. An algorithm that predicts optimal machining parameter-levels based on mathematical model should be developed, to reduce the need for costly and time consuming experiments.

CHAPTER THREE

METHODOLOGY

3.1 Introduction

This chapter covers the steps and procedures used in the study so as to meet the outlined objectives. Description of used materials and equipment is also presented. Preliminary experimental investigations and design of experiments process are also presented in this chapter. Finally, this chapter discusses the optimization process using Taguchi method.

3.2 Description of Materials Used for Experimentation

The Inconel-625 material was used for specimen in experimental work. According to the designer of AWT6S wire EDM machine used for cutting, the thickness can be set to 10, 20, 30, 40 and 50 mm. However, in this study, 10 mm thick specimen was selected for cost minimization. Photograph of specimen used is shown in Figure 3.1.



Figure 3.1: Specimen used for experimentation

Consumable brass wire of 0.25 mm diameter was used for cutting the material for surface roughness testing. Brass wire is widely used in Wire EDM processes due to its high tensile strength and high electrical conductivity Banker et al. (2013). Photograph of the 0.25 mm diameter roll of brass cutting wire is shown in Figure 3.2.



Figure 3.2: Photograph of brass cutting wire rolls

The dielectric fluid used in experimental work is de-ionised water due to its low viscosity and rapid cooling rate Popa et al. (1866). Photograph of de-ionized water tanks are shown in Figure 3.3.



Figure 3.3: Photograph of de-ionized water tanks

3.3 Experimental Setup

The experiments were carried out in machine workshops and methodology labs available in Jomo Kenyatta University of Agriculture and Technology (JKUAT). AWT6S EDM ①, PJ311 profile projector ② and MITUTOYO SJ-30 surface roughness tester ③ were used for the experimental work. Equipment used in the study are shown in Figure 3.4.



Figure 3.4: Equipment used for experimentation

The study includes experimental investigation where specimens were machined using the wire EDM machine, the surface roughness was measured using MITUTOYO SJ-30 surface roughness tester and the kerf width was measured using MITUTOYO PJ311 profile. The specifications of these equipment are shown in Table 3.1.

Table 3.1: Specifications of equipment used for experimentation

Equipment	Specifications	
Wire EDM	Model	AWT6S
	Dielectric fluid	De-ionized water
	t_{on} range (μs)	0.005-1.2
	t_{off} (μs)	1-50
	f_w range (mm/min)	1-15
Surface roughness tester	v_g (V)	20-150
	Model	PJ-301
Profile projector	Model	PJ-311
	Screen diameter (mm)	300
	Rotation (degrees)	360

3.3.1 Machining Process Using AWT6S Wire EDM Machine During Preliminary Experimentation

The AWT6S wire EDM machine utilizes a continuously travelling wire electrode to erode material from the workpiece (Inconel-625) submerged in dielectric fluid (de-ionized water). Referring to surface measurement standard as shown Table B.1 of Appendix B, 12.5 mm long straight cuts were performed for surface roughness testing and kerf width measurement. The specimens were clamped in the working table and the code for cutting was uploaded to initiate the machining process. Photograph of AWT6S wire EDM machine during sparking process is shown in Figure 3.5.



Figure 3.5: Set up for cutting process using AWT6S wire EDM machine

Schematic block diagram for functional setup of AWT6S wire EDM machine is shown in Figure 3.6.

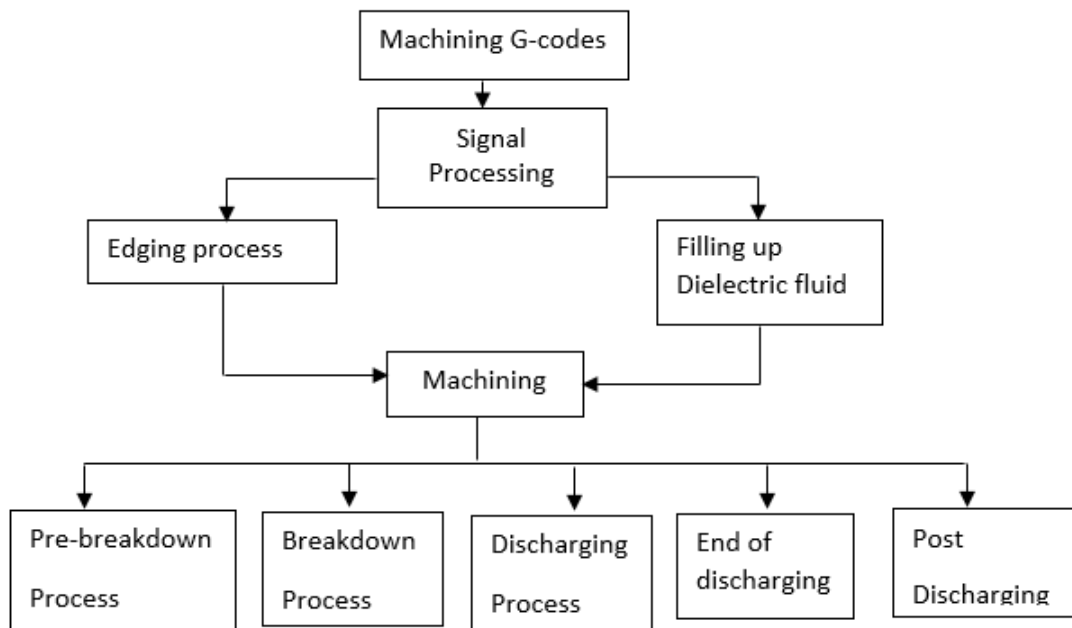


Figure 3.6: Schematic block diagram for functional setup of AWT6S wire EDM machine

Figure 3.6 shows the schematic block diagram for functional setup of AWT6S wire EDM machine. The G-codes are generated by the user and then inserted in the machine for signal processing. Edging process and filling up of dielectric fluid are performed for

machining initiation, which is performed in five steps namely, pre-breakdown phase, breakdown phase, discharge process, end of discharge phase and post discharge phase Sahu (2012). These steps are well discussed in section 1.6.

3.3.2 Surface Roughness Measurement Using MITUTOYO SJ-30 Surface Roughness Tester

Surface roughness is one of the important parameters used to test the suitability of a material for a certain application. Rough surfaces are more vulnerable to cracks and corrosion and therefore wear out faster than smoother surfaces K. Kumar et al. (2009). In this study, the MITUTOYO SJ-30 surface roughness tester was used to test the quality of surface finish. Photograph of MITUTOYO SJ-30 surface roughness tester is shown in Figure 3.7.



Figure 3.7: Set up for measuring surface roughness using MITUTOYO SJ-30 surface roughness tester

The surface roughness was measured by applying the average surface roughness (R_a) method referring to the *JSB0601-2001 and ISO* standard Yamazaki (1998), as

indicated in Appendix B.

Schematic block diagram for functional setup of MITUTOYO SJ-30 surface roughness tester is shown in Figure 3.8.

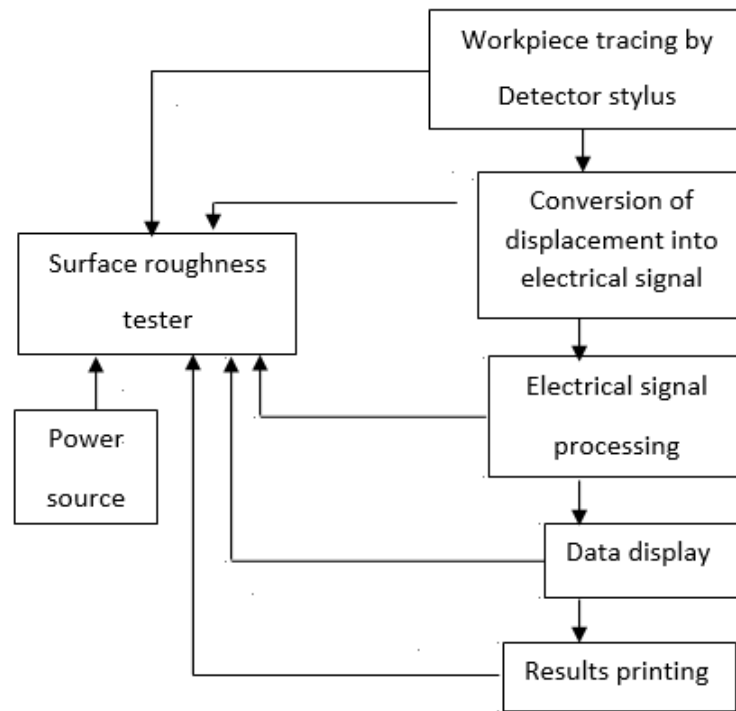


Figure 3.8: Schematic block diagram for setup of MITUTOYO SJ-30 surface roughness tester

Figure 3.8 shows the schematic block diagram for functional setup of MITUTOYO SJ-30 surface roughness tester. The detector stylus traces the workpiece surface and the vertical stylus displacement produced while tracing the workpiece surface is converted into electrical signals which are subjected to various calculation processes. The calculated results are displayed on the touch panel and the measured statistical data is printed out (Chen and Wang (2012)).

3.3.3 Measurement of Kerf Width Using PJ311 Profile Projector

In wire electrical discharge machining, the kerf width is the space left after the cutting wire has gone through the workpiece. The photograph of the PJ311 profile projector used to measure the kerf width is shown in Figure 3.9.

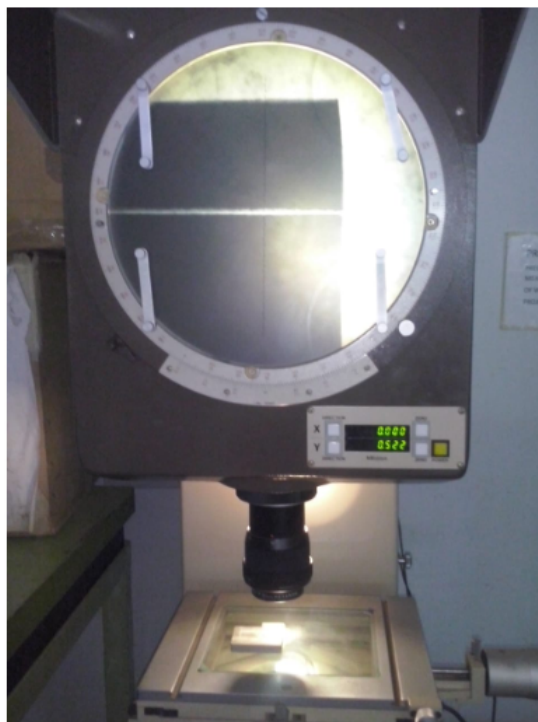


Figure 3.9: Set up for measuring kerf width using PJ311 profile projector

Schematic block diagram for functional setup of setup of PJ311 profile projector is shown in Figure 3.10.

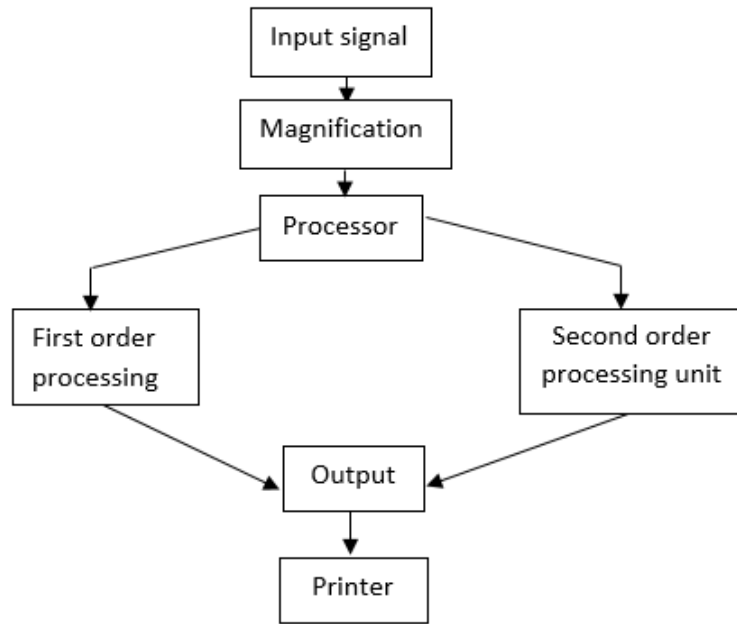


Figure 3.10: Schematic block diagram for setup of PJ311 profile projector

Figure 3.10 shows schematic block diagram for functional setup of PJ311 profile projector. The input signal is magnified and then sent to the processor for data recording and processing. Once information is processed from first and second order processing units, it is sent as an output to be printed Ali et al. (n.d.).

3.3.4 Calculation of Material Removal Rate

The material removal rate MRR , was calculated as Karsh and Singh (2018):

$$MRR = \frac{lwk}{t} \quad (3.1)$$

Where l is the length of cut (mm), w is the thickness of the specimen (mm), k is the kerf width (mm) and t is the machining time (min). These parameters are labeled as shown in Figure 3.11.

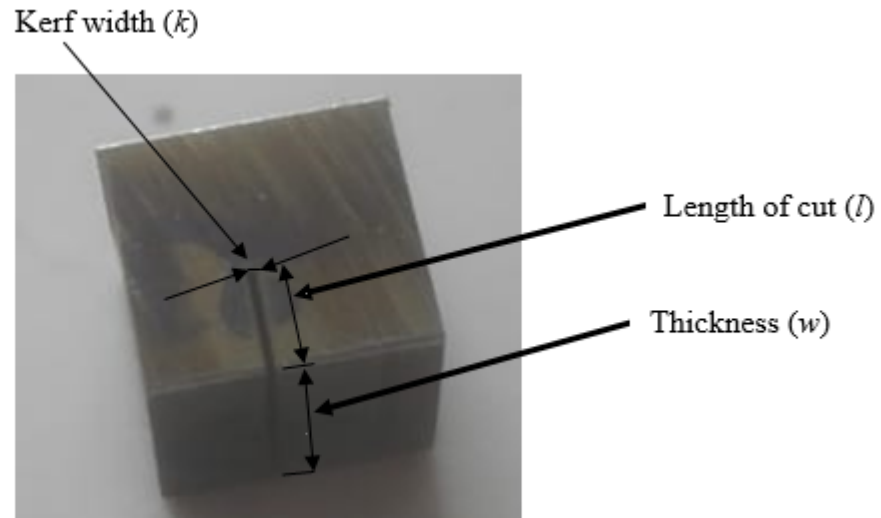


Figure 3.11: Photograph of Inconel-625 specimen used in the Study

3.4 Design of Experiments

3.4.1 Determination of Parameter Levels

In order to determine the standard parameter-levels to use in the study, preliminary investigations on the effect of input parameters were carried out.

The effect of pulse-on time on the machining process was investigated by varying the levels of this parameter from $0.005 \mu\text{s}$ to $1.2 \mu\text{s}$, although machining started from $0.4 \mu\text{s}$ as shown in Table C.1 of Appendix C, and keeping constant the levels of wire feed rate and gap voltage. For the wire feed rate, machining was performed in the range between 6 mm/min and 10 mm/min, holding constant the pulse-on time and gap voltage. For all the cases throughout the entire range, the wire feed rate was obtained minimum at 8 mm/min. The gap voltage was kept constant at 65 V, a value that had been reported to yield high surface finish for Inconel-X750, which has similar properties to Inconel-625 M. Kumar and Singh (2018). Machining was found stable between $0.4 \mu\text{s}$

and 0.6 μs , with minimum surface roughness at 0.5 μs .

The effect of gap voltage on the machining process was investigated by varying this parameter from 20 V to 150 V, Table C.2 of Appendix C, and keeping wire feed rate and pulse-on time constant at 8 mm/min and 0.5 μs respectively. To minimize the number of experiments, an increment of 2 V to 3 V was kept between two successive levels of gap voltage and the machining process was stable within 53 V and 68 V with minimum surface roughness for a gap voltage of 62 V.

The effect of wire feed rate was studied by keeping the pulse-on time and gap voltage constant at 0.5 μs and 62V respectively, and varying the wire feed rate from 1 mm/min to 15 mm/min, as shown in Table C.3 of Appendix C. The cutting process was found with less wire breakages between 6 mm/min and 10 mm/min. The parameter-levels resulting from preliminary investigations were selected for data set, as shown in Table C.4 and C.5 of Appendix C, based on the range that was observed to produce stable machining process, as shown in Table 3.2.

Table 3.2: Parameter-levels used

Factor	Parameter	Level		
1	Pulse-on time (μs)	0.4	0.5	0.6
2	Wire feed rate (mm/min)	6	8	10
3	Gap voltage (V)	56	62	68

3.4.2 Determination of Number of Experiments

The experiments were designed using Taguchi orthogonal array design of experiments (DOE). This technique involves variation in the process via the robust design of experiment which helps to investigate how different parameters affect variance and mean of process performance characteristics for optimization. The technique uses or-

thogonal arrays to arrange parameters affecting the process to decide the levels at which parameters should be set. Taguchi technique tests the pairs of combinations to help identify the factors that, with minimal experimentation, affect the product quality thus helping to save time and resources Roy (2001). The input parameters investigated in this work include pulse-on time, wire feed rate and gap voltage. All the other parameters were kept constant at their optimal levels as reported by previous researchers. Application of the analysis of variance (ANOVA) helped determine how each input parameter contribute to the process. Optimum machining performance is obtained by calculating the signal to noise (S/N) ratio. Smaller-is-better for surface roughness, given by:

$$\frac{S}{N}_{sr} = -10\log \left[\frac{1}{n} \sum_{i=1}^n Y_i^2 \right] \quad (3.2)$$

Larger-is-better for material removal rate, given by:

$$\frac{S}{N}_{mrr} = -10\log \left[\frac{1}{n} \sum_{i=1}^n \frac{1}{Y_i^2} \right] \quad (3.3)$$

Norminal-is-the best for combined material removal rate and optimum surface roughness shown as follows:

$$\frac{S}{N}_{sr,mrr} = 10\log \left[\frac{\bar{Y}^2 - \frac{\sigma^2}{n}}{\sigma^2} \right] \quad (3.4)$$

Where Y_i represents the response of the given factor level combination, \bar{Y} represents the mean of responses for a given factor level combination, σ stands for the standard deviation of the responses of a given factor level combination, and n represents the number of responses in the factor level combination.

Before determination of the number of experiments to be conducted, the degrees of freedom was calculated to determine the possible number of ways the system can vary with respect to the parameter levels. Degree of freedom DOF , for each parameter was calculated as:

$$DOF = S_K - 1 \quad (3.5)$$

And the total degree of freedom DOF_{tot} , was calculated as:

$$DOF_{tot} = \sum_{i=1}^k [S_{ki} - 1] \quad (3.6)$$

Where S_k represents the number of levels while k stands for the number of factors.

Each parameter was assigned three levels (Level 1, Level 2, and Level 3). Assigned parameter-levels and respective calculated degrees of freedom are shown in Tables 3.3 and 3.4.

Table 3.3: Assigned parameter-levels

Parameter	Level		
	Level 1	Level 2	Level 3
Pulse-on time	A 1	A 2	A3
Wire feed rate	B 1	B 2	B3
Gap voltage	C 1	C 2	C3

Table 3.4: Calculation of degrees of freedom

Factor	Level	DOF
Pulse-on time	3	3-1=2
Wire Feed rate	3	3-1=2
Gap Voltage	3	3-1=2
Pulse-on time*Wire feed rate	-	(3-1)*(3-1)=4
Pulse-on time* Gap voltage	-	(3-1)*(3-1)=4
Wire feed rate * Gap voltage	-	(3-1)*(3-1)=4
Total DOF	$\sum_{i=1}^k [S_{ki} - 1]$	18

The number of experiments N_{exp} , was determined as:

$$N_{exp} = 1 + \sum_{i=1}^k [S_{ki} - 1] = 19 \quad (3.7)$$

The most suitable orthogonal array is one that would cater for at least 19 experiments, without considering noise factors. In Taguchi design of experiments method, if all interactions and noise factors are considered, the number of experiments N_{exp} , is calculated as:

$$N_{exp} = p^n \quad (3.8)$$

Where n represents the number of levels.

In this work, three parameters each with three levels were considered. Therefore, twenty seven experiments obtained using Taguchi L_{27} orthogonal array were sufficient for experimentation.

3.4.3 Analysis of Variance for Parameter Levels

Analysis of variance (ANOVA) refers to a technique used to determine variation of parameter levels. In this method, analysis of means is carried out to determine if individual factor-level means are different from the mean of all observations. Minitab-17 $\text{\textcircled{R}}$ was used to perform analysis of means using the following steps:

Step 1. Computation of the mean at each factor level

The average of observations at each factor level, \bar{y}_i , ($i = 1, \dots, r$), was calculated as:

$$\bar{y}_i = \frac{\sum_{j=1}^{n_i} y_{ij}}{n_i} \quad (3.9)$$

Where y_{ij} are observations at i, j^{th} factor levels, n_i represents the number of observations at the i^{th} factor level.

Step 2. Computation the grand mean of all observations

The grand mean of \bar{y}_i across factor levels was calculated as:

$$\bar{y} = \frac{\sum_{i=1}^r \bar{y}_i}{r} \quad (3.10)$$

Where \bar{y} stands for the average of observations at each factor level (grand mean) and $r =$ number of factor levels.

Step 3. Computation of an estimated standard deviation of observation

An estimate of the standard deviation S_i , was calculated as:

$$S_i = \sqrt{\frac{\sum_{j=1}^{n_i} (y_{ij} - \bar{y}_i)^2}{n_i - 1}} \quad (3.11)$$

Step 4. Calculation of the standard deviation for an estimate of the variation of the observations

The standard deviation S_p , for an estimate of the variation of the observations was

calculated as:

$$S_p = \sqrt{\frac{\sum_{i=1}^r [(n_i - 1) S_i^2]}{n_T - r}} \quad (3.12)$$

Where n_T stands for total number of observations.


Step 5. Computation of the upper and lower decision limits

The upper and lower decision limits were calculated based on the level numbers in the factor and the observation number of as:

$$UDL = \bar{y} + h_\alpha s_p \sqrt{\frac{r-1}{rn_1}} \quad (3.13)$$

$$LDL = \bar{y} - h_\alpha s_p \sqrt{\frac{r-1}{rn_1}} \quad (3.14)$$

Where,

UDL and LDL are respectively the upper and lower decision limits, n_1 is the number of observations at each level, and h_α is the statistical test value between 0.001 and 0.1 Nelson (1983), corresponding to the optimum level as obtained from Minitab-17 .

3.5 Optimization of Machining Process Using Taguchi

Method

Procedure of Taguchi optimization process is shown in the flow chart shown in Figure 3.12 Shah et al. (2013).

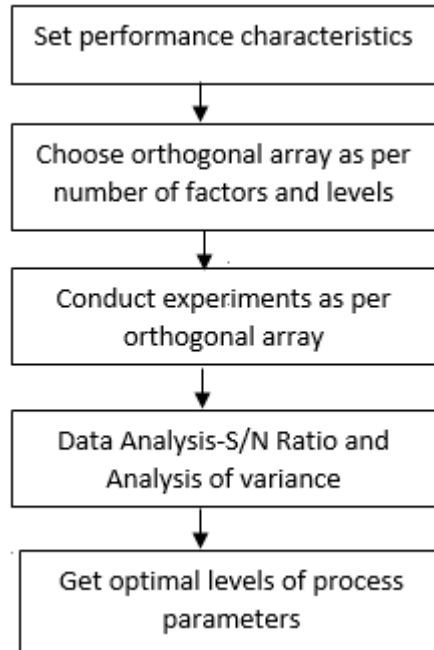


Figure 3.12: Procedure for Taguchi Optimization Process

In order to investigate the effect of combined input parameters on output performance, the parameter-levels were selected after preliminary experimental investigations. After selecting factors and levels, Taguchi design of experiments method was applied to select L_{27} orthogonal array. Experiments were then conducted by setting parameter-levels to their corresponding values as it was shown in Table 3.2.

The pulse-on time, wire feed rate and gap voltage were selected as process factors, whereas the surface roughness and material removal rate were selected as response characteristics. The means and signal to noise ratio were set to analyze Taguchi design. The S/N ratios were calculated from equations 3.2, 3.3 and 3.4. For optimization, individual desirability technique was applied Jeong and Kim (2009).

For maximization, desirability is calculated as:

$$\left\{ \begin{array}{ll} d_i = 0; & \text{for } \hat{y}_i < L_i \\ d_i = \left[\frac{\hat{y}_i - L_i}{T_i - L_i} \right]^{r_i}; & \text{for } L_i \leq \hat{y}_i \leq T_i \\ d_i = 1; & \text{for } \hat{y}_i > T_i \end{array} \right. \quad (3.15)$$

For minimization, the desirability is calculated as:

$$\left\{ \begin{array}{ll} d_i = 0; & \text{for } \hat{y}_i < U_i \\ d_i = \left[\frac{U_i - \hat{y}_i}{U_i - T_i} \right]^{r_i}; & \text{for } T_i \leq \hat{y}_i \leq U_i \\ d_i = 1; & \text{for } \hat{y}_i > T_i \end{array} \right. \quad (3.16)$$

For optimization of two performance measures compromising one another, the desirability is calculated as:

$$\left\{ \begin{array}{ll} d_i = \left[\frac{\hat{y}_i - L_i}{T_i - L_i} \right]^{r_i}; & \text{for } L_i \leq \hat{y}_i \leq T_i \\ d_i = \left[\frac{U_i - \hat{y}_i}{U_i - T_i} \right]^{r_i}; & \text{for } T_i \leq \hat{y}_i \leq U_i \\ d_i = 0; & \text{for } \hat{y}_i < L_i \\ d_i = 0; & \text{for } \hat{y}_i > U_i \end{array} \right. \quad (3.17)$$

Where \hat{y}_i represents the predicted value of i^{th} response, T_i represents the target value for i^{th} response, L_i represents lowest acceptable value for i^{th} response, U_i represents highest acceptable value for i^{th} response, d_i stands for desirability for i^{th} response and r_i stands for weight of desirability function of i^{th} response. In the current study, the compromising performance measures are the material removal rate and surface roughness.

3.5.1 Response Tables

Response tables were generated for mean and signal to noise ratio to indicate which factor has the highest influence on the response. The following steps are performed to generate response tables:

1. The Mean and signal to noise ratio for each factor level combination are calculated.
2. At each level the average of the response characteristic for each factor is calculated.
3. The delta value for each factor is calculated as:

$$DV = \left[\frac{\sum_{j=1}^{n_i} y_{ij}}{n_i} \right]_{high} - \left[\frac{\sum_{j=1}^{n_i} y_{ij}}{n_i} \right]_{low} \quad (3.18)$$

Where DV is the delta value.

The rank, which is the order of the delta values from high to low, is calculated.

Factors are assigned ranks 1, 2 and 3 from the highest to the lowest delta values.

3.6 Summary

As shown in this chapter, 10 mm thick plates of Inconel-625, brass wire and de-ionized water are the materials used for experimentation. AWT6S wire EDM machine was used for cutting the material, MITUTOYO SJ-30 surface roughness tester was used for measuring surface roughness, while PJ311 profile projector was used for measuring kerf width. Preliminary experimental investigations were performed to come up with parameter-levels. Taguchi L_{27} orthogonal array was used for experimentation and mathematical model was developed to correlate pulse-on time, wire feed rate and gap voltage with surface roughness and material removal rate. An algorithm was developed for prediction of optimal control parameters from the model. Finally, optimization was performed using Taguchi optimization technique.

CHAPTER FOUR

RESULTS AND DISCUSSION

4.1 Introduction

The results of the influence of input parameters on output performance measures, the models used for prediction, graphical user interface, comparison between predicted and experimental results, response surface methodology, analysis of variance and Taguchi optimization process are discussed in this chapter.

4.2 Investigation on the influence of input process parameters to machining process

Results from preliminary investigations are discussed in this section.

a. Influence of Pulse-on time on Machining Process

The influence of pulse-on time on surface roughness and material removal rate was examined by plotting the data mean for levels using the main effects plot technique in Mintab-17 [®], as shown in Figures 4.1 and 4.2.

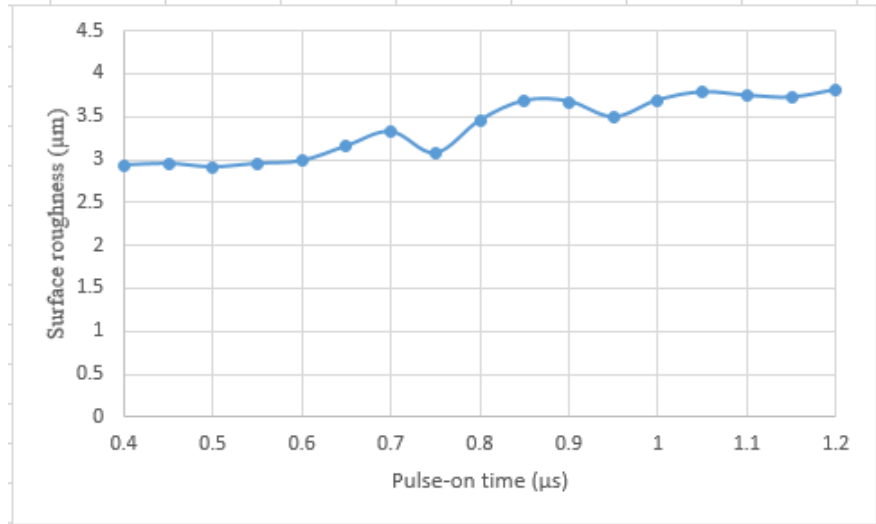


Figure 4.1: Effect of pulse-on time on surface roughness

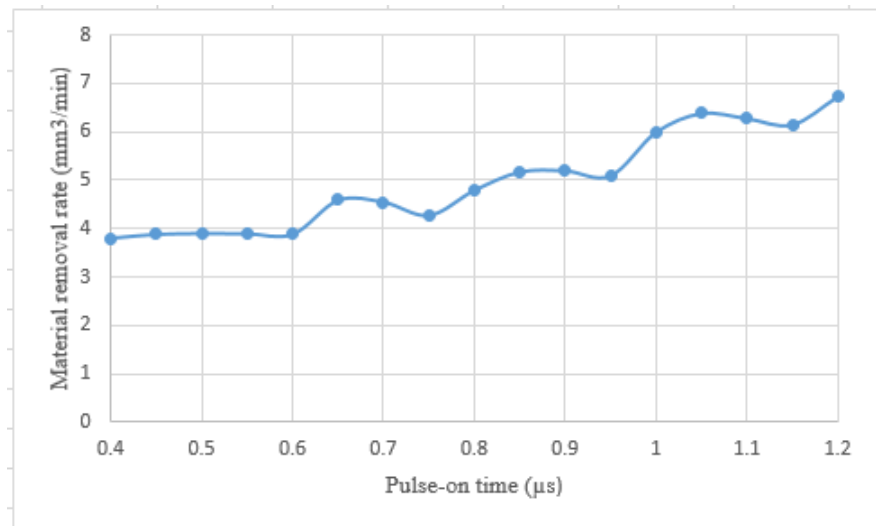


Figure 4.2: Effect of pulse-on time on material removal rate

From Figures 4.1 and 4.2, it can be seen that both surface roughness and material removal rate increase with the increase in pulse-on time. It can also be seen that the cutting process started from $0.4 \mu\text{s}$. This could be due to the fact that small pulses between $0.005 \mu\text{s}$ and $0.4 \mu\text{s}$ are not enough to initiate the sparking process in the spark gap. It is also observed that, between $0.4 \mu\text{s}$ and $0.6 \mu\text{s}$, a range that was observed to produce stable cutting process, the minimum surface roughness and maximum material

removal rate are found at pulses of $0.5 \mu\text{s}$, meaning that in the combination of the three input process parameters, there is a possibility of reducing the surface roughness and increasing the material removal rate with this level.

b. Influence of Gap Voltage on Machining Process

The influence of gap voltage on surface roughness and material removal rate is shown in Figures 4.3 and 4.4, respectively.

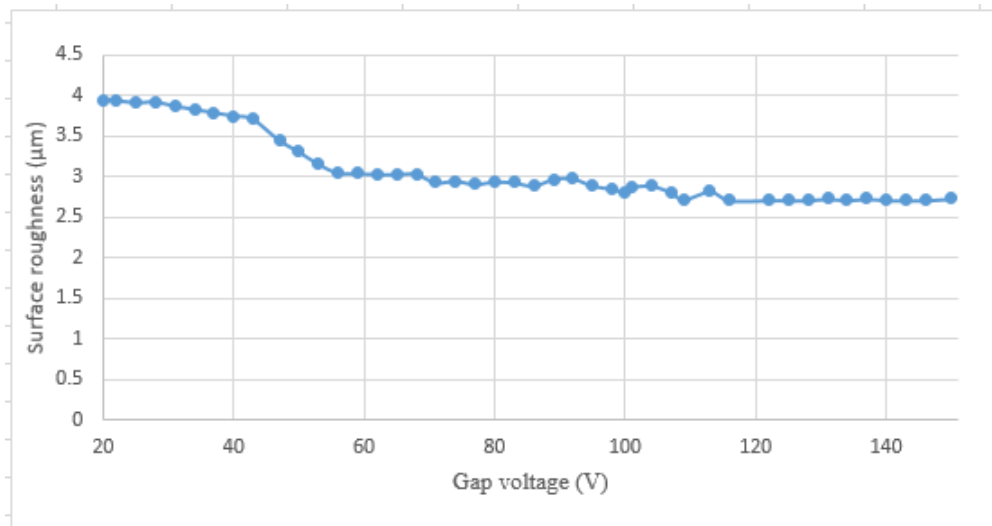


Figure 4.3: Effect of gap voltage on surface roughness

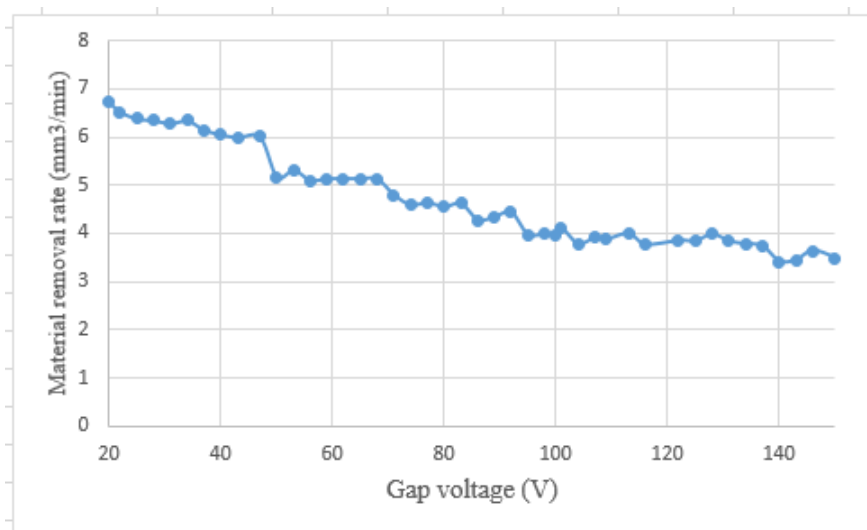


Figure 4.4: Effect of gap voltage on material removal rate

It can be seen that both surface roughness and material removal rate decrease with the increase in gap voltage. Within the range with stable machining which is between 53 V and 68 V, the minimum surface roughness and maximum material removal rate are observed at 62 V. This means that, this level may have a remarkable influence in combination with pulse-on time and wire feed rate. However, it can be observed that the surface roughness changes only in small proportions after a certain gap voltage. This could be due to the fact that the smaller the value of gap voltage the faster the discharge speed, ending up with instability of machining. Below 56 V, there is a significant change in surface roughness and material removal rate because the machining was unstable.

c. Influence of Wire Feed Rate on Machining Process

The effect of wire feed rate on surface roughness and material removal rate are shown in Figures 4.5 and 4.6.

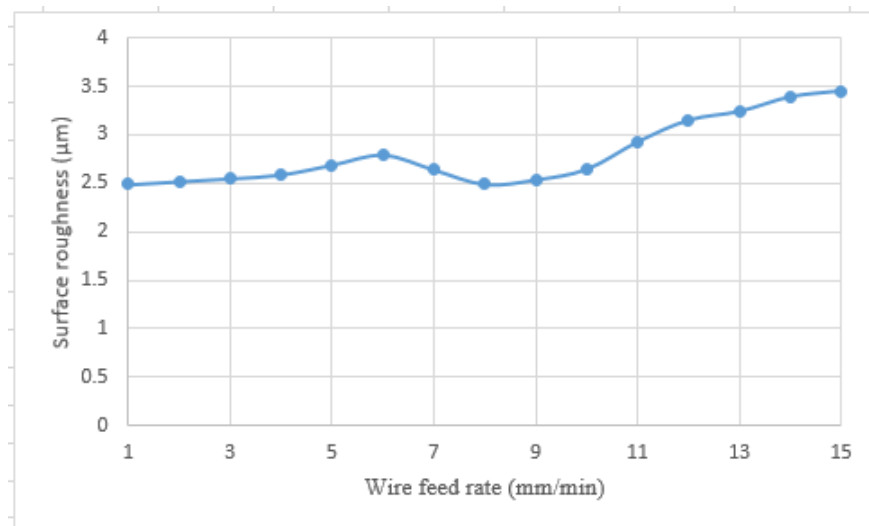


Figure 4.5: Effect of wire feed rate on surface roughness

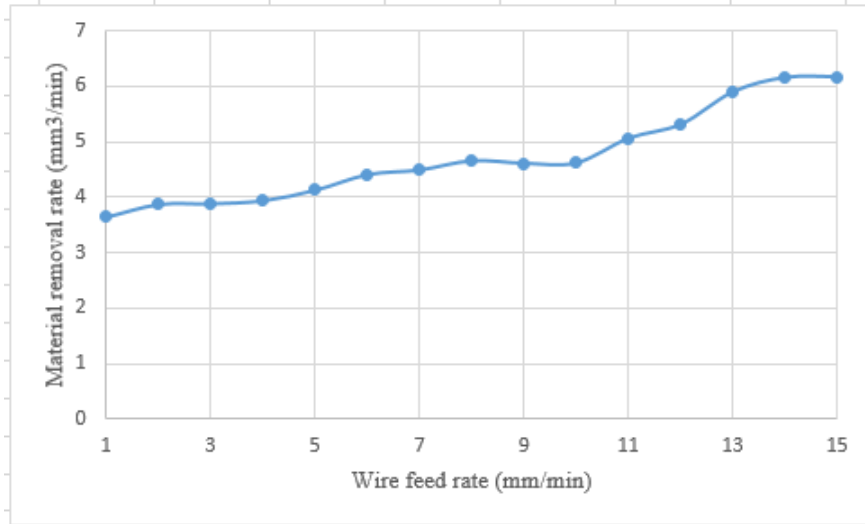


Figure 4.6: Effect of wire feed rate on material removal rate

It can be observed that both surface roughness and material removal rate increase with the increase in wire feed rate, with a tendency of reduction in surface roughness and increase in material removal rate for wire feed rates of between 6 mm/min and 10 mm/min. This means that, minimum surface roughness and material removal rate can be obtained if the wire feed rate is set within this range.

d. Rank of influence of inputs parameters to machining process

By applying Taguchi optimization technique, Tables 4.1 and 4.2 were generated from MINITAB-17 [®] to find out the effect of each level of process parameter on surface roughness and material removal rate.

Table 4.1: Response Table for means surface roughness

Parameter	t_{on}	f_w	v_g
	2.896	3.155	3.202
<i>SR</i>	3.027	2.980	2.958
	3.267	2.995	2.880
Rank	1	2	3

From Table 4.1, the assigned ranks show that the pulse-on time is the most influential parameter followed by the wire feed rate and the gap voltage.

Table 4.2: Response table for means material removal rate

Parameter	t_{on}	f_w	v_g
	8.379	8.016	7.730
<i>MRR</i>	8.027	7.830	8.069
	7.596	8.155	8.202
Rank	1	3	2

From Table 4.2, the assigned ranks indicate that the most influential parameter is pulse-on time followed by the gap voltage and the wire feed rate.

4.3 Models for Material Removal Rate and Surface roughness

Multiple regression was carried out using MINITAB-17 [®] software to predict optimal performance measures. Predicted output reading obtained from the model is shown in Table D.1 of Appendix D.

Generated model for surface roughness (*SR*), is given as:

$$\begin{aligned}
 SR = & 2.356225t_{on}^2 + 0.00058081f_w^2 + 0.000001166v_g^2 + 2.44065t_{on} \\
 & + 0.038319f_w - 0.0017172v_g + 0.073987t_{on}f_w - 0.0033156t_{on}v_g \\
 & - 0.000052056f_wv_g + 0.632025
 \end{aligned} \tag{4.1}$$

Generated model for material removal rate (MRR), is given as:

$$\begin{aligned}
MRR = & 1.223236t_{on}^2 + 0.0000937024f_w^2 + 0.0000294849v_g^2 + 4.273584t_{on} \\
& + 0.3740352f_w - 0.02098152v_g + 0.02141216t_{on}f_w - 0.01201116t_{on}v_g \quad (4.2) \\
& - 0.0001051248f_wv_g + 3.732624
\end{aligned}$$

From the model for surface analysis and material removal rate, it can be seen that the coefficients for f_w^2 , v_g^2 , v_g , $t_{on}v_g$ and f_wv_g are very small. This means that low levels of the wire feed rate and the gap voltage, and the interaction of either the pulse-on time or the wire feed rate with the gap voltage are less significant to surface roughness and material removal rate, leading to simplified model as:

$$SR = 2.356225t_{on}^2 + 2.44065t_{on} + 0.038319f_w + 0.073987t_{on}f_w + 0.632025 \quad (4.3)$$

$$\begin{aligned}
MRR = & 1.223236t_{on}^2 + 4.273584t_{on} + 0.3740352f_w - 0.02098152v_g \\
& + 0.02141216t_{on}f_w - 0.01201116t_{on}v_g + 3.732624 \quad (4.4)
\end{aligned}$$

Where,

t_{on} is the pulse-on time in (μs), f_w is the wire feed rate in (mm/min) and v_g is the gap voltage in (V).

The models shown in equation 4.3 and 4.4 can be used for prediction of the effect of pulse-on time, wire feed rate and gap voltage on surface roughness and material removal rate in wire EDM of Inconel-625.

4.3.1 Comparison between predicted and experimental surface roughness and material removal rate

Predicted and experimental values showing the effect of input process parameters on surface roughness and material removal rate are shown from Figures 4.7 to 4.12.

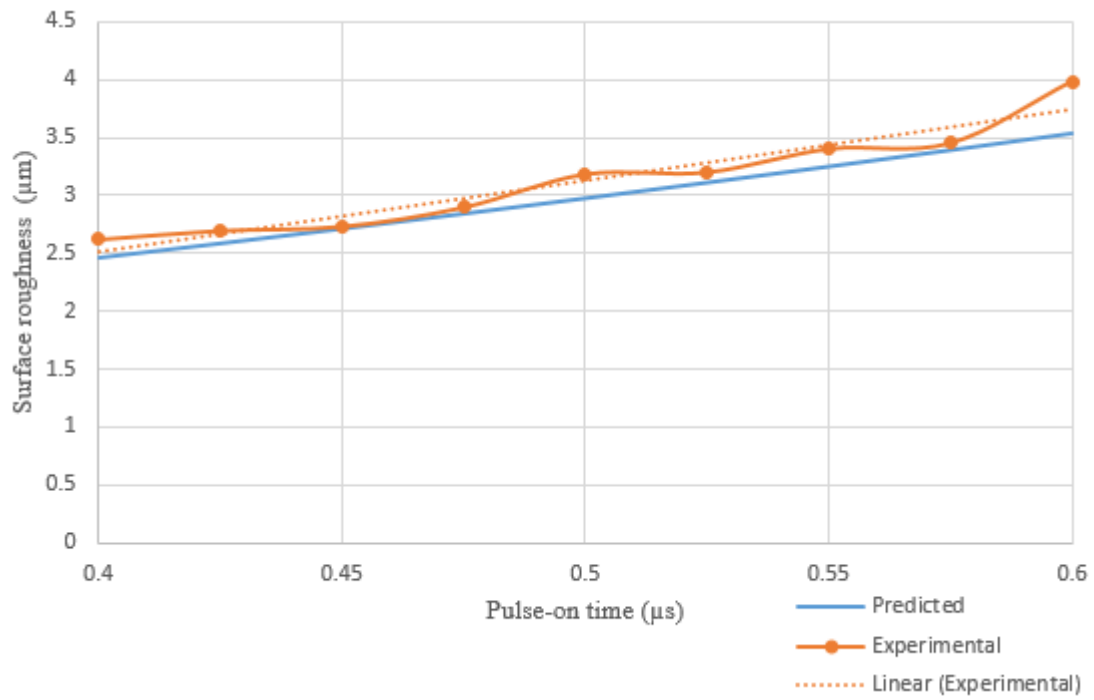


Figure 4.7: Predicted and experimental surface roughness against pulse-on time

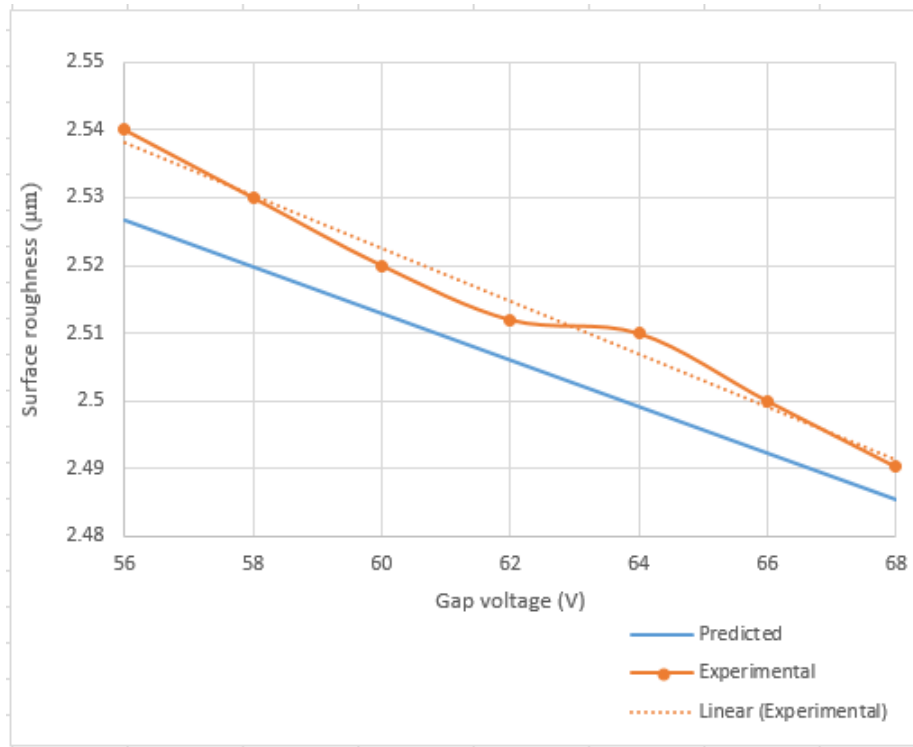


Figure 4.8: Predicted and experimental surface roughness against gap voltage

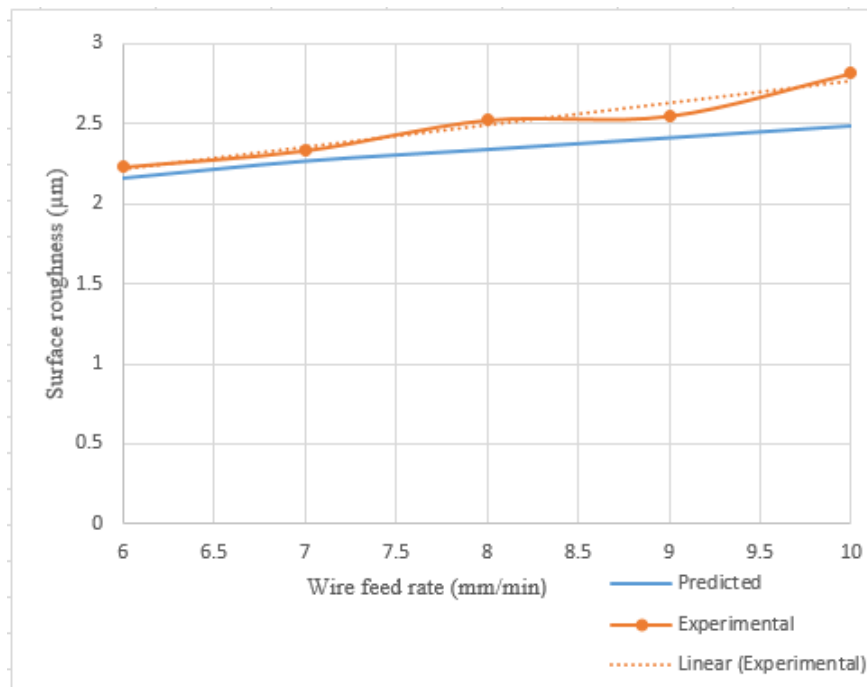


Figure 4.9: Predicted and experimental surface roughness against wire feed rate

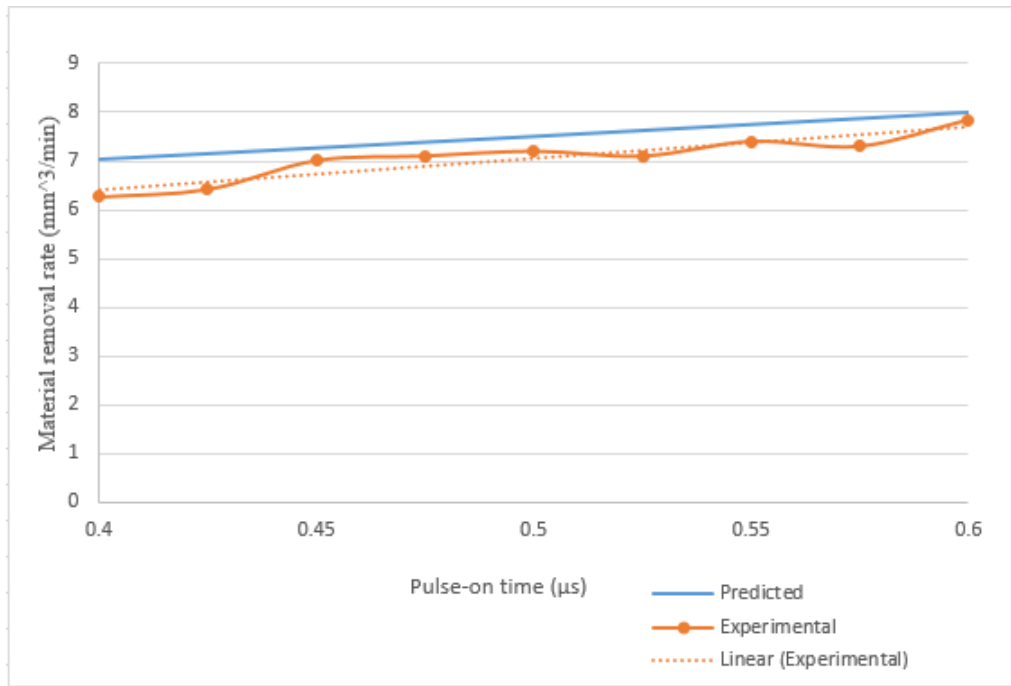


Figure 4.10: Predicted and experimental material removal rate against pulse-on-time

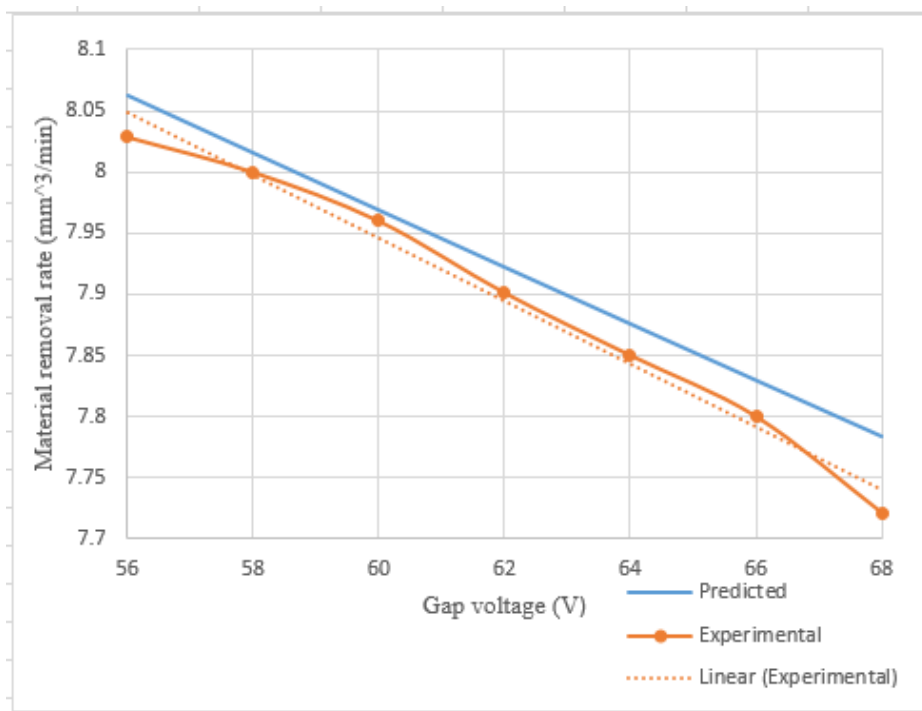


Figure 4.11: Predicted and experimental material removal rate against gap voltage

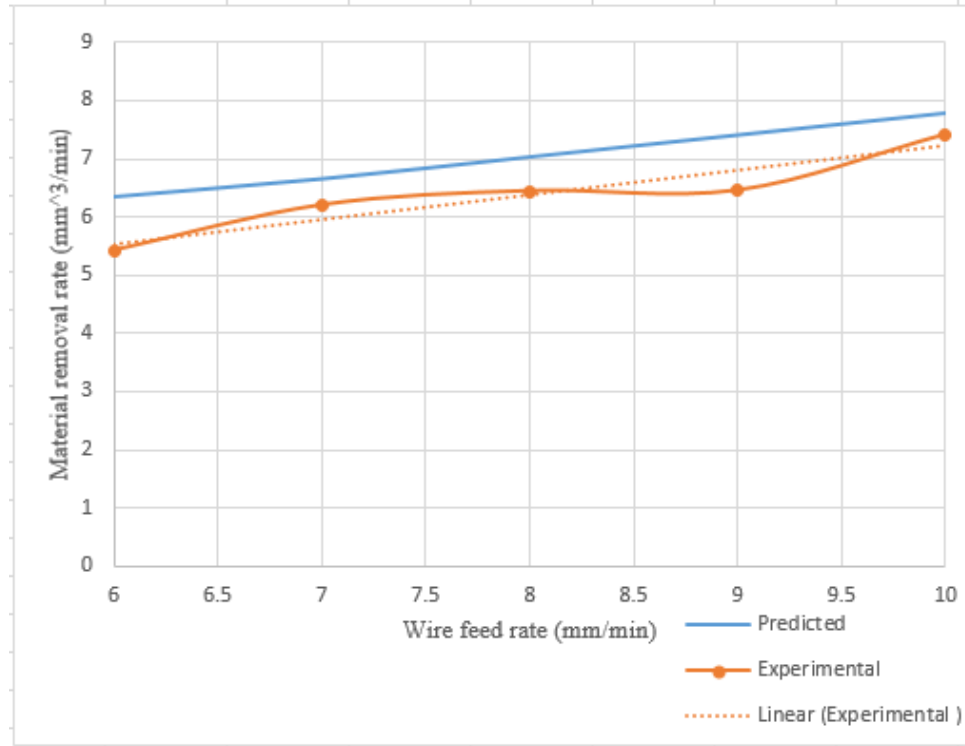


Figure 4.12: Predicted and experimental material removal rate against wire feed rate

The graphs shown from Figures 4.7 to 4.12 show that predicted and experimental results do have almost similar profiles. This means that the models used for prediction are accurate. The largest difference between predicted and experimental readings is found to be $0.4432 \mu\text{m}$ and $0.7660 \text{ mm}^3/\text{min}$ for surface roughness and material removal rate, respectively, for pulse-on time. This could be due to the highest influence of this parameter on the process. However, this is not the calculated standard deviation for the model, considering all parameters together. It can also be seen that for surface roughness, experimental values are slightly higher than predicted minimum values, whereas for material removal rate, experimental values are lower than predicted maximum values. This could be caused by the parameter-interaction effect. Model diagnostic checking is a method used to analyze the model residuals based on certain

assumptions in order to confirm the accuracy of the model. The diagnostic checking assumption was done by building a normal probability plot of the residuals, where every residual is plotted versus its expected value under normality. In this diagnostic it is expected to obtain a straight line plot, with emphasized central points than the extremes, indicating that the residual distribution is normal Ghodsiyeh, Davoudinejad, Hashemzadeh, Hosseininezhad, and Golshan (2013); Nourbakhsh et al. (2013). RSM was adopted for analyzing data, normal plot of RSM model residuals for surface roughness is shown in Figure 4.13.

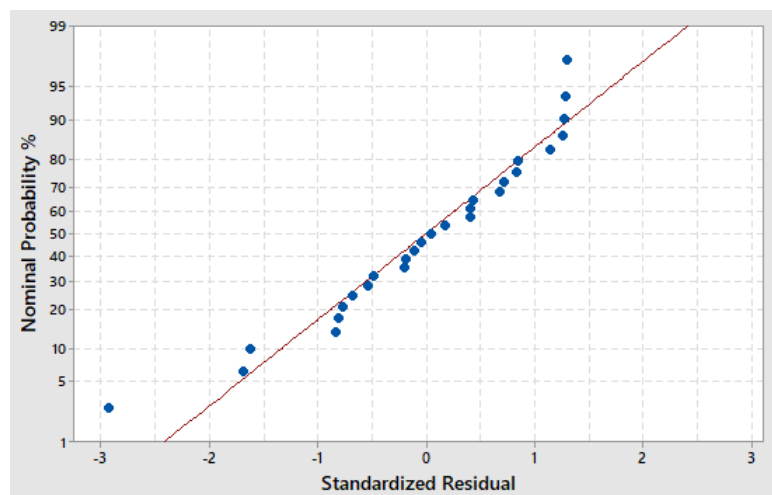


Figure 4.13: Normal plot of the RSM model residuals for surface roughness

The nominal plot of the RSM model residuals for material removal rate is shown in Figure 4.14.

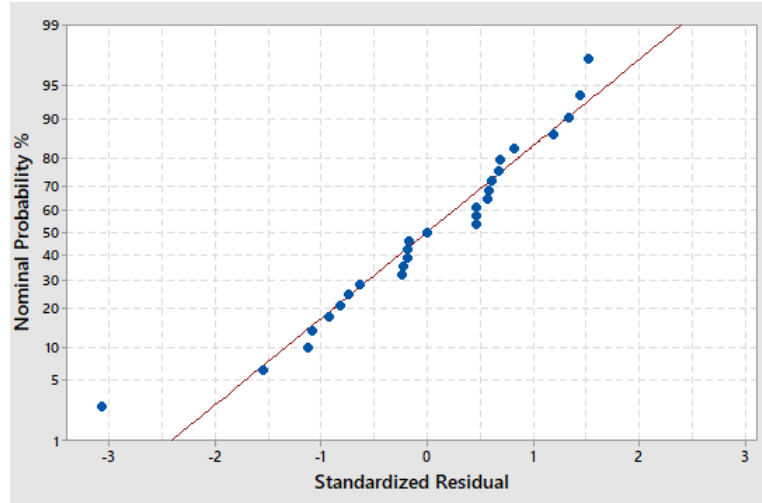


Figure 4.14: Normal plot of the RSM model residuals for material removal rate

Figures 4.13 and 4.14 show the normal plot of the RSM model residuals for surface roughness and material removal rate, respectively. The obtained results indicate that the errors are distributed normally because the residuals fall on a straight line, showing that the developed model fits the data well.

4.4 Graphical User Interface

A graphical user interface was developed on the basis of developed models that correlate input machining characteristics with output performance measures. The interface displays optimum machining conditions based on desired output performance as desired by the user. A screenshot of the user interface and sample of generated machining conditions are shown in Figure 4.15.

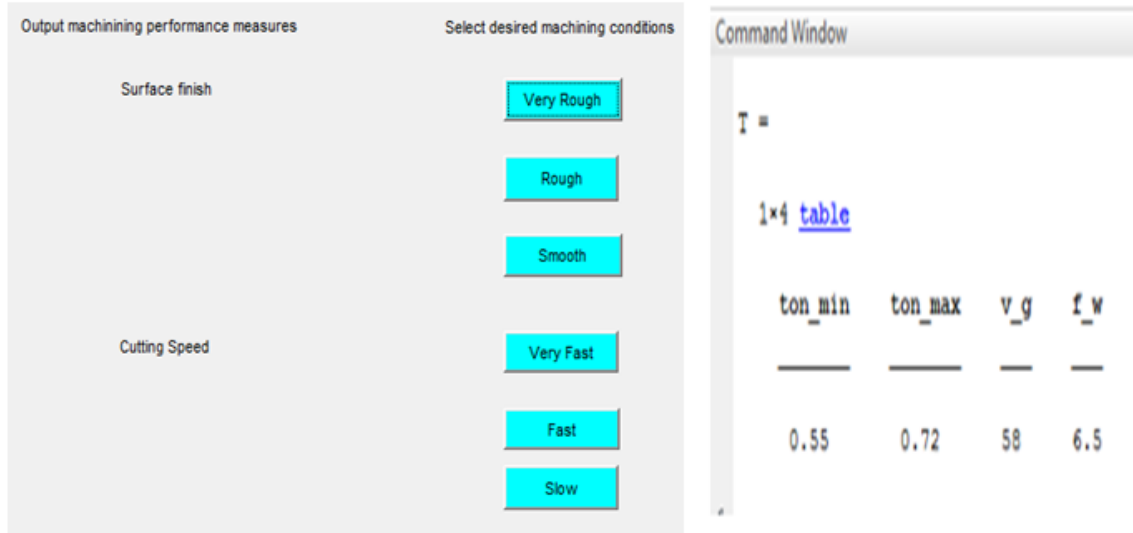


Figure 4.15: Screenshot of the user interface and output

Optimal machining conditions for machining of Inconel-625 using wire EDM, brass wire and de-ionised water, as dielectric fluid, are shown in Table 4.3.

Table 4.3: Optimal machining conditions

Parameter	Surface roughness			Material removal rate		
	Very rough	Rough	Smooth	Very fast	Fast	Slow
t_{on} min (μs)	0.55	0.42	0.07	0.41	0.28	0.07
t_{on} max (μs)	0.72	0.52	0.44	0.71	0.39	0.31
f_w (mm/min)	6.5	8.92	7	8.6	9.33	10
V_g (V)	58	64.30	59	64.4	62	68

Table 4.3 shows a summary of optimal machining conditions for desired output performance. For example, it can be seen that when a smooth surface roughness is needed, the user is suggested to select a pulse-on time between $0.07 \mu s$ and $0.44 \mu s$, wire feed rate of 7 mm/min and a gap voltage of 59 V . When a very fast material removal rate is needed, the user should select a pulse-on time between $0.41 \mu s$ and $0.71 \mu s$, wire feed rate of 8.6 mm/min and a gap voltage of 64.4 V . This shows that the developed user interface eliminates costly and time consuming experiments that could

be conducted for every output performance needed.

4.5 Response Surface Methodology Analysis

The Response Surface Methodology based on central composite design was used for evaluation of the effect of pulse-on time, wire feed rate and gap voltage on surface roughness and material removal rate. Two control parameters at a time were considered for analyzing the interaction between them using surface contour plots and the influence of two parameters on machining output was analyzed using response surface plots.

4.5.1 Surface Contour Plots for Surface Roughness and Material Removal Rate

The analysis of the influence of pulse-on time, wire feed rate and gap voltage on surface roughness and material removal rate was done using surface contour plots. The contour plots show how the values of the surface roughness and material removal rate change as a function of two variables of the input process parameters, while the third variable is held constant Baş and Boyacı (2007).

a. Contour plot for pulse-on time, gap voltage and surface roughness

Contour plot of the relationship between pulse-on time, gap voltage and surface roughness is shown in Figure 4.16.

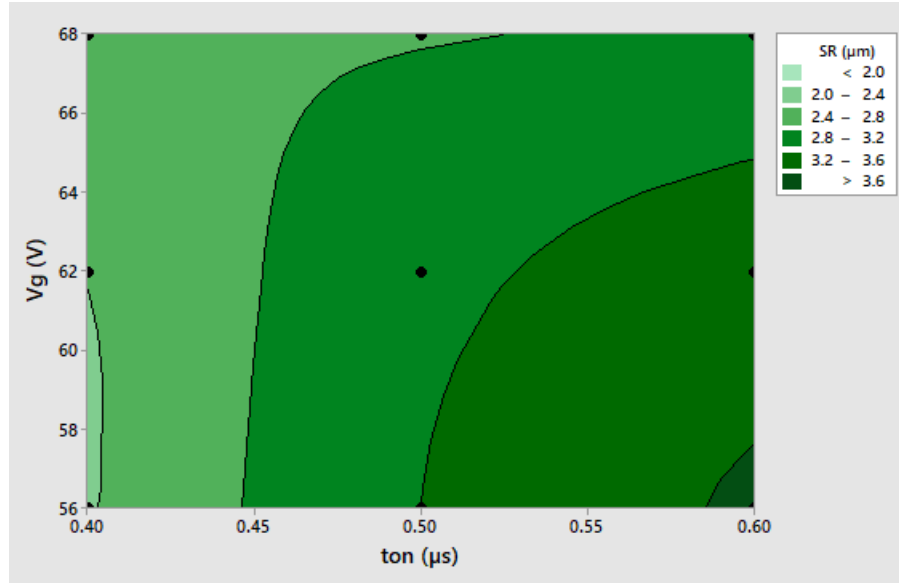


Figure 4.16: Contour Plot of surface roughness against gap voltage and pulse-on time

Figure 4.16 presents the contour plot of the relationship between pulse-on time, gap voltage and surface roughness. It can be seen that, at low values of pulse-on time of between 0.4 and 0.45 μs , even when the gap voltage is increased to it's maximum level of 68 V, the surface roughness remains between 2 and 2.4 μm . Maintaining the values of gap voltage and increasing the values of pulse-on time, the surface roughness increases from 2 μm to 3.6 μm . At low values of gap voltage and high values of pulse-on time, the surface roughness increases. At high values of gap voltage and high values of pulse-on time, the surface roughness still increases. This means that the effect of gap voltage is less significant to the surface roughness and that in the interaction of pulse-on time and gap voltage, the pulse-on time is the most influential parameter on the surface roughness. The maximum surface roughness is obtained for higher pulse-on time and lower gap voltage, whereas the lower surface roughness is obtained for lower pulse-on time and higher gap voltage.

b. Contour plot for pulse-on time, wire feed rate and surface roughness

Contour plot of the relationship between pulse-on time, wire feed rate and surface roughness is shown in Figure 4.17.

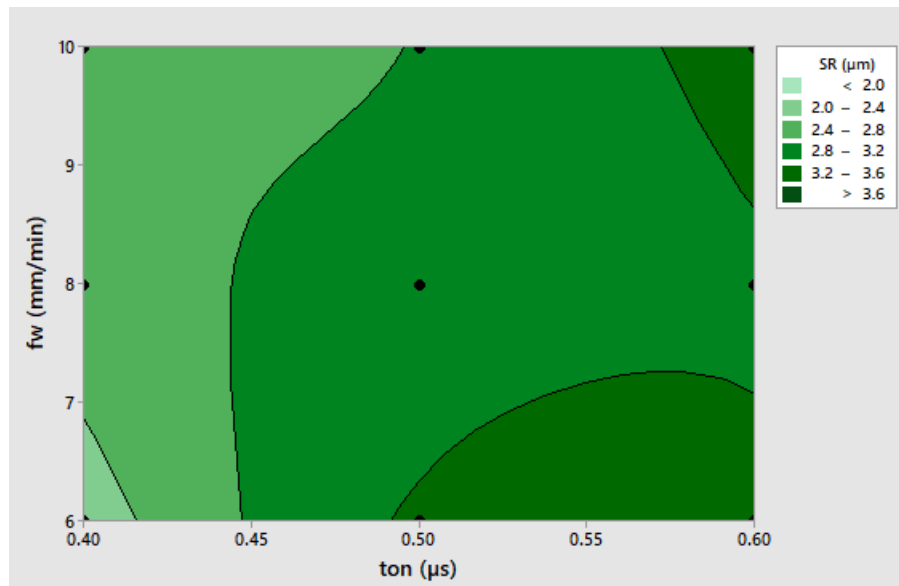


Figure 4.17: Contour Plot of surface roughness against wire feed rate and pulse-on time

Figure 4.17 presents the contour plot of the relationship between parameters pulse-on time, wire feed rate and surface roughness. It can be seen that, at low values of pulse-on time even when the wire feed rate is increased to its maximum, the surface roughness does not increase. Maintaining the values of wire feed rate and increasing the values of pulse-on time, the surface roughness increases. At low values of wire feed rate and high values of pulse-on time, the surface roughness increases. At high values of wire feed rate and high values of pulse-on time, the surface roughness still increases. This means that the effect of wire feed rate is less significant to the surface roughness and that in the interaction of pulse-on time and wire feed rate, the pulse-on time is the most influential parameter on the surface roughness. The maximum surface roughness

is obtained for higher pulse-on time and higher wire feed rate, whereas the minimum surface roughness is obtained for lower pulse-on time and lower wire feed rate.

c. Contour plot for gap voltage, wire feed rate and surface roughness

Contour plot of the relationship between gap voltage, wire feed rate and surface roughness is shown in Figure 4.18.

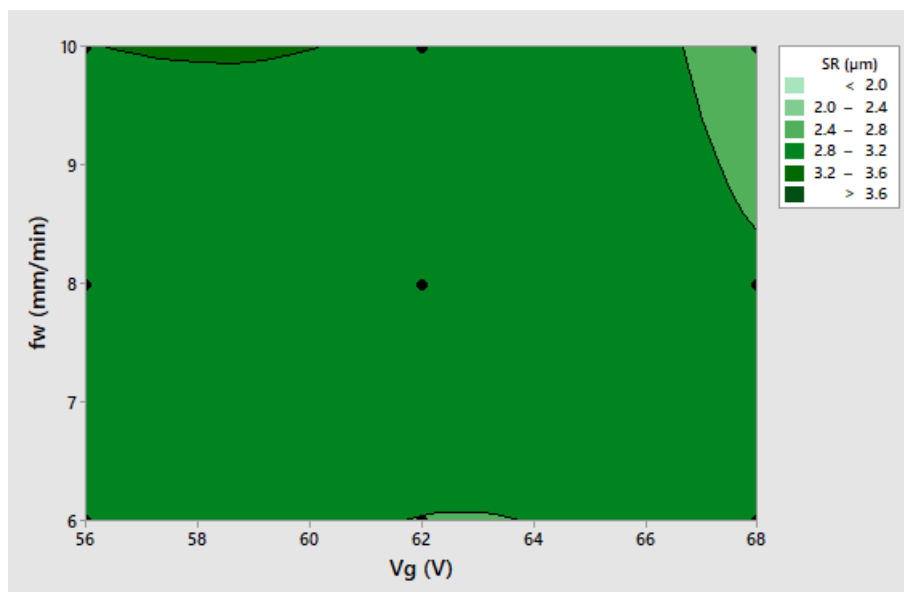


Figure 4.18: Contour Plot of surface roughness against wire feed rate and gap voltage

Figure 4.18 shows the contour plot for gap voltage, wire feed rate and surface roughness. It can be seen that as the gap voltage increases from 56 V, keeping the wire feed rate at low values, the surface roughness falls between 2.8 μm and 3.2 μm until the gap voltage reaches about 62 V. It can also be seen that the surface roughness reduces up to levels of between 2.0 μm and 2.4 μm until the gap voltage reaches 64 V, from which the surface roughness raises again. This means that in the combination of gap voltage and wire feed rate, the gap voltage adds less significant effect on the surface roughness. When the wire feed rate is increased up to its maximum and as

the gap voltage increases, the surface roughness increases up to the levels of between $3.2 \mu\text{m}$ to $3.6 \mu\text{m}$. This value falls again to the levels of between $2.8 \mu\text{m}$ and $3.2 \mu\text{m}$ for the gap voltage of between 60 V and 66 V, after which the surface roughness drops again between $2.0 \mu\text{m}$ and $2.4 \mu\text{m}$. Keeping constant the gap voltage at low values and increasing the wire feed rate up to about 9.7 mm/min, the surface roughness increases up to the levels of between $3.2 \mu\text{m}$ and $3.6 \mu\text{m}$. This means that in the combination of wire feed rate and gap voltage, the wire feed rate is the most influential parameter. The maximum surface roughness is obtained for higher wire feed rate and lower gap voltage, whereas the minimum surface roughness is obtained for higher gap voltage and wire feed rate.

d. Contour plot for pulse-on time, wire feed rate and material removal rate

Contour plot of the relationship between pulse-on time, wire feed rate and material removal rate is shown in Figure 4.19.

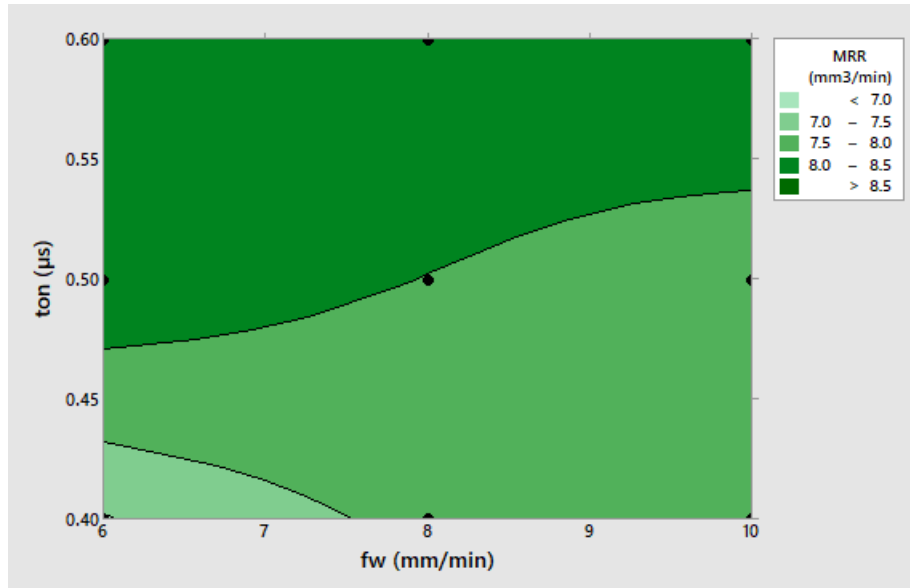


Figure 4.19: Contour Plot of material removal rate against wire feed rate and pulse-on time

Figure 4.19 shows the contour plot of wire feed rate and pulse-on time against material removal rate. It can be seen that, at low values of pulse-on time, the material removal rate falls between $7.0 \text{ mm}^3/\text{min}$ and $7.5 \text{ mm}^3/\text{min}$. This value increases up to the levels of between $7.5 \text{ mm}^3/\text{min}$ and $8.0 \text{ mm}^3/\text{min}$, from the value of wire feed rate of about $7.5 \text{ mm}/\text{min}$. When the pulse-on time is increased to its maximum, the material removal rate is between $8.0 \text{ mm}^3/\text{min}$ and $8.5 \text{ mm}^3/\text{min}$. Within the entire interval of the wire feed rate, the material removal rate increases with the increase in pulse-on time. This means that, in this combination of pulse-on time and material wire feed rate, the pulse-on time is the most influential parameter on material removal rate. The maximum material removal rate is obtained for higher pulse-on time, whereas the minimum material removal rate is obtained for lower pulse-on time and lower wire feed rate.

e. Contour plot for pulse-on time, gap voltage and material removal

rate

Contour plot of the relationship between pulse-on time, gap voltage and material removal rate is shown in Figure 4.20.

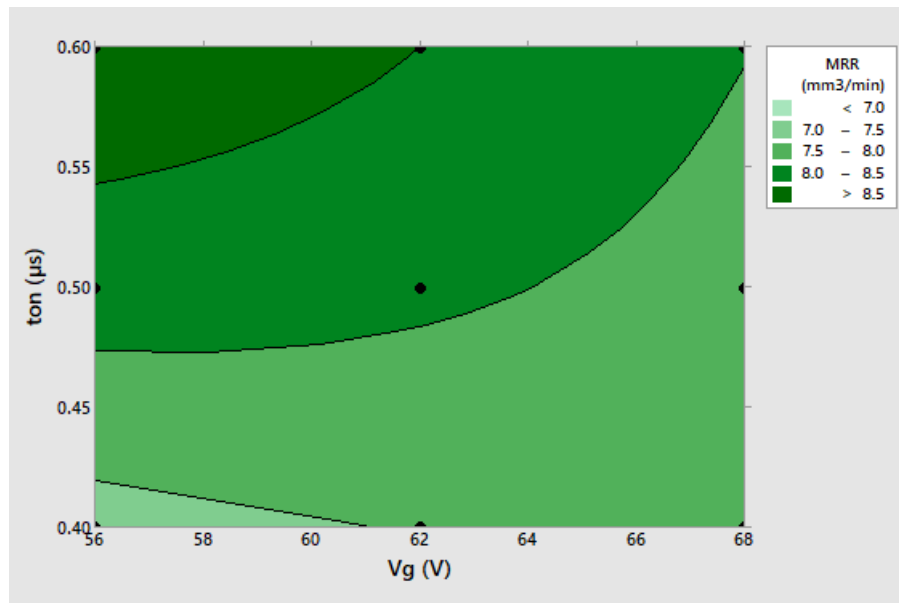


Figure 4.20: Contour Plot of material removal rate against gap voltage and pulse-on time

Figure 4.20 shows the contour plot of material removal rate against gap voltage and pulse-on time. It can be seen that at low values of the pulse-on time, the material removal rate starts increasing from 7.0 mm³/min to the levels of between 7.0 mm³/min and 7.5 mm³/min, when the gap voltage reaches about 61 V. It can also be seen that throughout the entire interval of the gap voltage, the material removal rate increases with the increase in pulse-on time. This means that, in the combination of pulse-on time and gap voltage, the pulse-on time is the most influential parameter on the material removal rate. The maximum material removal rate is obtained for higher levels of pulse-on time and lower levels of gap voltage, whereas the minimum material removal rate is obtained for lower pulse-on time and higher gap voltage.

f. Contour plot for wire feed rate, gap voltage and material removal rate

Contour plot of the relationship between wire feed rate, gap voltage and material removal rate is shown in Figure 4.21.

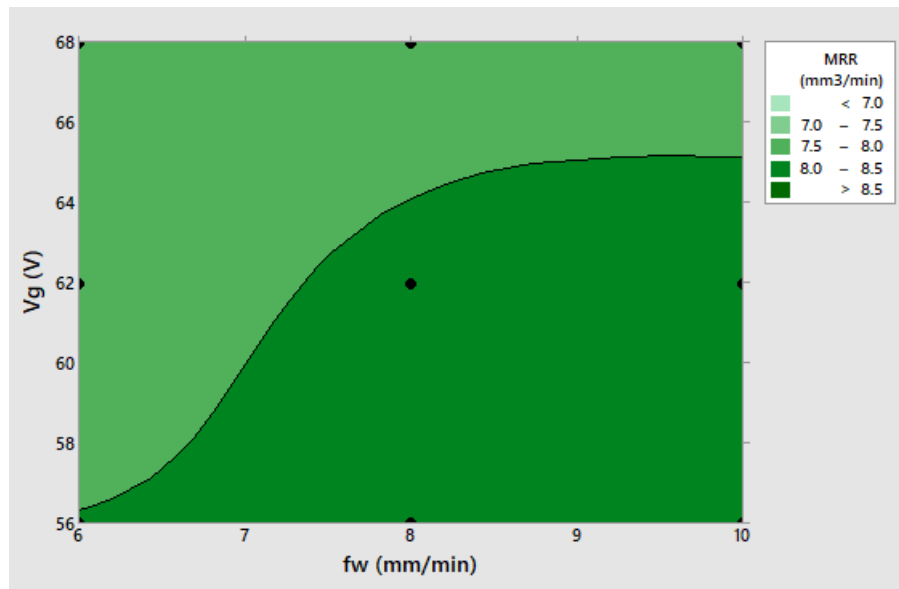


Figure 4.21: Contour Plot of material removal rate against gap voltage and wire feed rate

Figure 4.21 shows the contour plot of material removal rate against gap voltage and wire feed rate. It can be seen that for low values of the wire feed rate, the material removal rate does not change with the change in gap voltage. However, when the wire feed rate is increased to its maximum, the material removal rate reduces from the levels of between 8.0 mm³/min and 8.5 mm³/min to the levels of between 7.0 mm³/min and 7.5 mm³/min, when the value of gap voltage reaches about 65 V. For maximum gap voltage, the material removal rate does not change with the increase in wire feed rate. This means that in the combination of wire feed rate and gap voltage, the gap voltage is less influencing on the material removal rate.

It can be concluded that for the material removal rate, the most influential parameter is the pulse-on time, followed by the wire feed rate and gap voltage. The maximum material removal rate is obtained for higher wire feed rate and lower gap voltage, whereas the minimum material removal rate can be obtained for higher gap voltage.

4.5.2 Response Surface Plots for Performance Measures Against Input Parameters

In order to investigate the influence of input control parameters on output performance measures, response surface plots were generated and the effect of two parameters at a time on response was analyzed.

a. Response surface plot for pulse-on time, wire feed rate with surface roughness and material removal rate

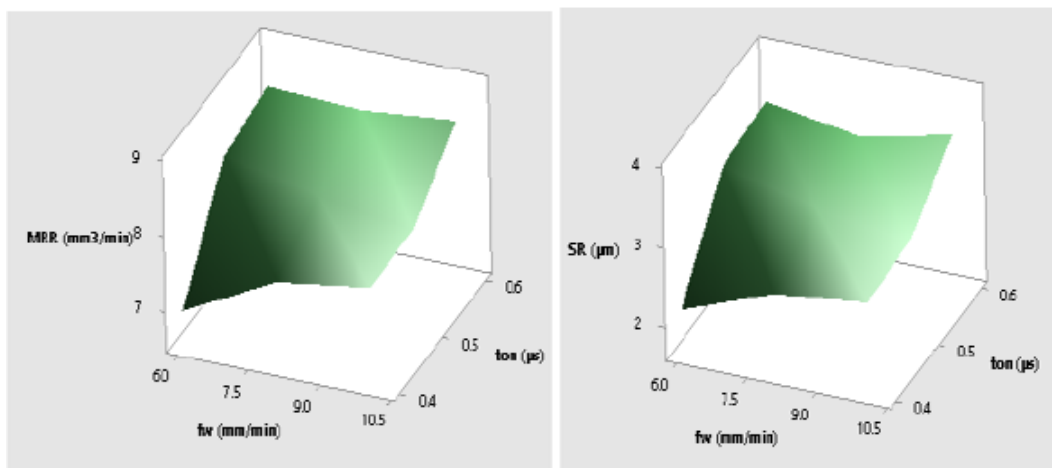


Figure 4.22: Response surface plot for pulse-on time, wire feed rate with surface roughness and material removal rate

Figure 4.22 shows the response surface plot of the pulse-on time and wire feed rate against surface roughness and material removal rate. It can be seen that for both responses, the gradient for pulse-on time and wire feed rate increases from lowest to

highest levels of these parameters. This implies that the surface roughness and material removal rate increase with the increase in both pulse-on time and wire feed rate.

b. Response surface plot for pulse-on time, gap voltage with surface roughness and material removal rate

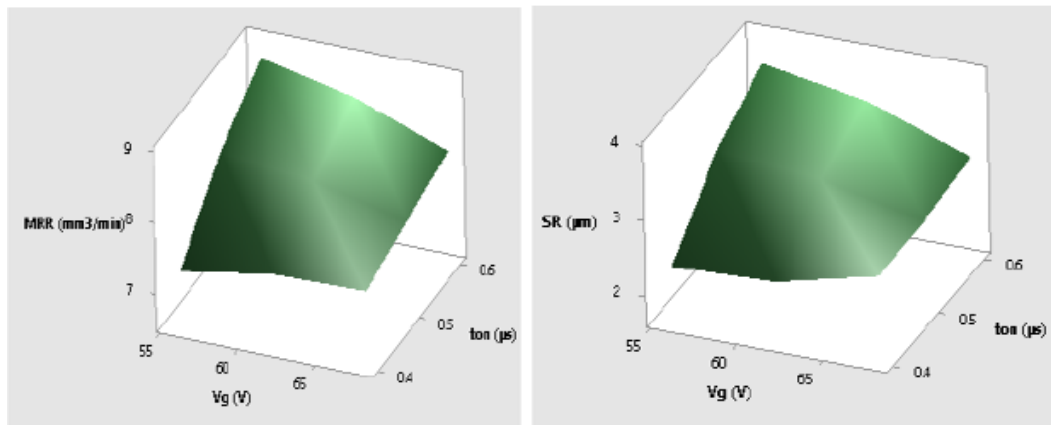


Figure 4.23: Response surface plot for pulse-on time, gap voltage with surface roughness and material removal rate

Figure 4.23 shows the response surface plot of the pulse-on time and gap voltage against surface roughness and material removal rate. For surface roughness, it can be seen that, the gradient at a pulse-on time of $0.6 \mu s$ is higher than the gradient at the pulse-on time of $0.4 \mu s$. It can also be seen that for the gap voltage, the gradient decreases with the increase in this parameter up to around $60 V$, where the gradient starts increasing. This could be due to the interaction between the increase in surface roughness as the pulse-on time increases and the decrease in surface roughness as the gap voltage increases. For material removal rate, it can be seen that for the pulse-on time, the gradient increases with this parameter. However, for the gap voltage, it can be seen that the gradient increases and then tends to decrease. This could be due to the interaction between

the increase in material removal rate as the pulse-on time increases and the decrease in material removal rate as the gap voltage increases.

c. Response surface plot for wire feed rate, gap voltage with surface roughness and material removal rate

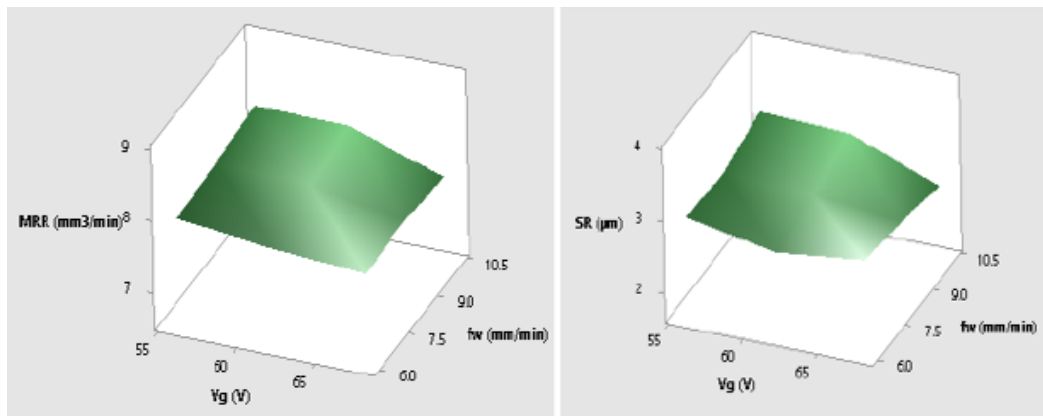


Figure 4.24: Response surface plot for wire feed rate, gap voltage with surface roughness and material removal rate

Figure 4.24 shows the response surface plot of the wire feed rate and gap voltage against surface roughness and material removal rate. For surface roughness, it can be seen that the gradient increases from lowest to highest levels for the wire feed rate, whereas the gradient decreases from the lowest to the highest for the gap voltage. This shows that the surface roughness increases with the increase in wire feed rate and decreases with the increase in gap voltage. The small deviation realised for the gap voltage profile could be caused by the trade-off between the influence of this parameter and the wire feed rate. For material removal rate, it can be seen that for the wire feed rate, the gradient increases from lowest to highest values of this parameter. However, gradient for the gap voltage tends to increase for the lower values and decreases for the higher values. This means that the decrease in material removal rate due to the increase in

gap voltage is affected by the increase in material removal rate due to the increase in the wire feed rate.

4.6 Analysis of Variance Results

After optimizing the machining process following Taguchi optimization technique, ANOVA tables were generated to show the significance of input parameters on the process. In analysis of variance, the total degrees of freedom (*DF*) are used to estimate the values of unknown population parameters. The sequential sum of squares (*Seq SS*) quantifies the amount of variation in the response data that is explained by each term as it is sequentially added to the model. The adjusted sums of squares (*Adj SS*) represent measures of variation for various components of a model. Adjusted mean squares (*Adj MS*) show variations of terms regardless of the order they were entered. The F-value (*F*) is used to determine whether the term is associated with the response. Minitab uses *DF*, *F*, *Adj MS*, *Seq SS*, and *Adj SS* to calculate the p-value for parameters of the model. In statistics, an input parameter is said to be statistically significant to the process if it's associated P-value is greater than 0.05, meaning 95% of significance Rice (1989). ANOVA results for means and S/N ratio for surface roughness and material removal rate are presented in Tables 4.4, 4.5, 4.6 and 4.7.

Table 4.4: ANOVA results for Means surafce roughness

Parameter	DF	Seq SS	Adj SS	Adj MS	F	P
t_{on}	2	2.2530	1.7531	0.87656	10.81	0.039
f_w	2	0.3622	0.4393	0.21967	2.71	0.046
v_g	2	0.5851	0.5851	0.29254	3.61	0.049
		S=0.2369 R-Sq=98.5%				

Table 4.5: ANOVA results for S/N ratios surface roughness

Parameter	DF	Seq SS	Adj SS	Adj MS	F	P
t_{on}	2	20.47	16.371	8.1856	9.34	0.023
f_w	2	3.993	4.836	2.4179	2.76	0.037
v_g	2	6.042	6.042	3.0212	3.45	0.048
S=0.1671 R-Sq=98.7%						

Tables 4.4 and 4.5 present ANOVA results for Means and S/N ratio surface roughness. The P-values for the pulse-on time is 0.039 and 0.023 for S/N ratio. This means that this parameter is significant to the process by 96.1 % and 97.7 % for means and S/N ratio respectively. For the wire feed rate, the P-value are 0.046 and 0.037 for means and S/N ratio, respectively. This means that the wire feed rate is significant to the means and S/N ratio surface roughness by 99.54 % and 99.63 %, respectively. The gap voltage is significant to both means and S/N ratio by 95.1 % and 95.2 %, respectively, since the corresponding P-values for means and S/N ratio are 0.049 and 0.048. It can be seen that for surface roughness, the pulse-on time is the most influential parameter followed by the wire feed rate and gap voltage. The standard deviation (S) is used to assess how far the data values fall from the fitted values. The lower value of the standard deviation, the better the model describes the response. The standard deviations of 0.2369 and 0.1671 for means and S/N ratio, respectively, are closer to zero. This shows that the model is accurate. R^2 shows the percentage of variation in the response. R^2 ranges from 0% to 100%, and it is used to determine how well the model fits data. The higher the R^2 value, the better the model fits data. The R^2 of 98.5% for means and 98.57% for S/N ratio show that the model fits well data.

Table 4.6: ANOVA results for means material removal rate

Parameter	DF	Seq SS	Adj SS	Adj MS	F	P
t_{on}	2	8.483	8.483	4.2416	16.57	0.0121
f_w	2	1.613	1.613	0.8063	3.15	0.0382
v_g	2	3.290	3.290	1.6452	6.43	0.0251
S=0.2367 R-Sq=97.6%						

Table 4.7: ANOVA results for S/N ratios material removal rate

Parameter	DF	Seq SS	Adj SS	Adj MS	F	P
t_{on}	2	7.482	7.472	4.2315	17.46	0.0171
f_w	2	1.512	1.714	0.7062	3.16	0.0422
v_g	2	3.281	3.291	1.5451	6.42	0.0242
S=0.3357 R-Sq=98.3%						

Tables 4.6 and 4.7 present ANOVA results for means and S/N ratio material removal rate. The P-values for the pulse-on time is 0.0121 and 0.0171 for S/N ratio. This means that this parameter is significant to the process by 98.79 % and 98.29 % for means and S/N ratio respectively. For the wire feed rate, the P-values are 0.0382 and 0.0422 for means and S/N ratio, respectively. This shows that the wire feed rate is significant to the means and S/N ratio surface roughness by 96.18 % and 95.78 %, respectively. For the gap voltage, P-values for means and S/N ratio are 0.0251 and 0.0242 which implies that this parameter is significant to the process by 97.49 % and 97.58 % for means and S/N ratio respectively. It can be seen that for material removal rate, the pulse-on time is the most influential parameter followed by the gap voltage and wire feed rate. The model for material removal rate is accurate since the standard deviations of 0.2367 and 0.3357, for means and S/N ratio, are closer to zero. The R^2 of 97.6% for means and 98.3% for S/N ratio show the fitness.

4.7 Optimization Using Taguchi Method

The main effects plot for means and S/N ratio for surface roughness are shown in Figures 4.25 and 4.26.

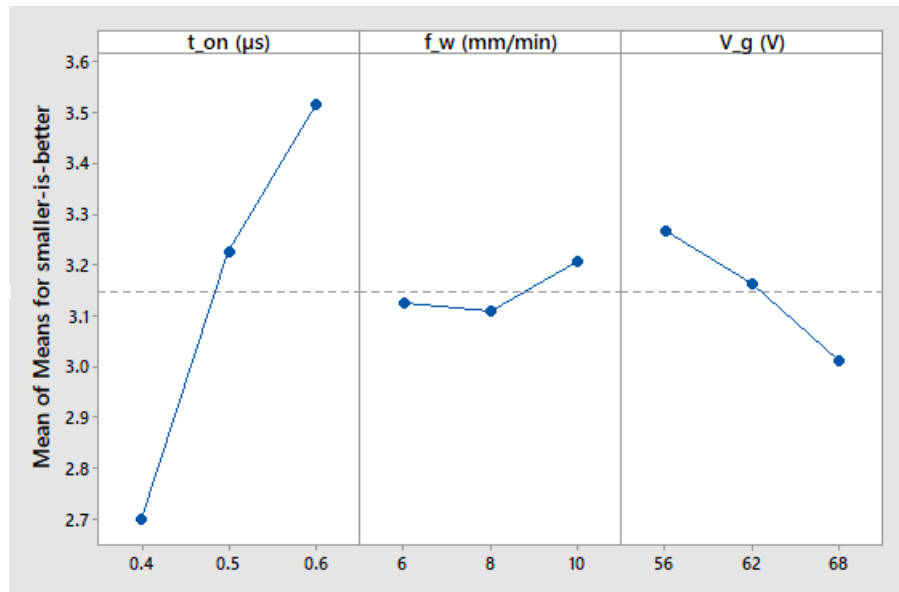


Figure 4.25: Main effects plot for Means of SR

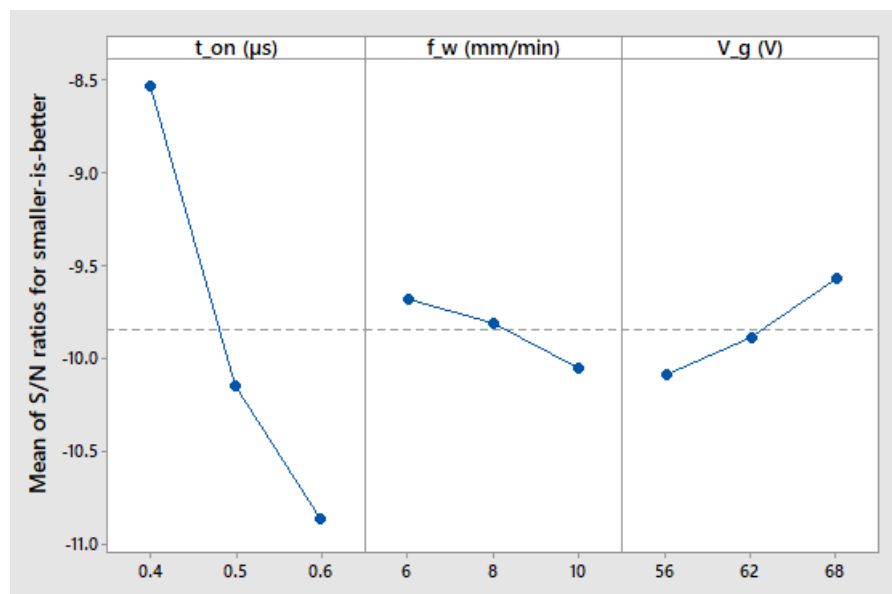


Figure 4.26: Main effects plot for S/N ratios of SR

Figures 4.25 and 4.26 show the main effect plots for means and S/N ratio surface

roughness. It can be seen that both the means and S/N ratios surface roughness are respectively minimized and maximized for the pulse-on time, wire feed rate and gap voltage of 0.4 μs , 8 mm/min and 68 V, respectively. It can be seen that the means surface roughness increases as the pulse-on time increases. The possible reason could be the fact that as the pulse-on time increases, there is an occurrence of pulse width caused by the higher peak discharge current to increase the roughness of the surface. It is also shown that the means surface roughness increases as the wire feed rate increases. This is due to creation of more discharges as the rate of feeding the cutting wire becomes larger and larger. There is a decrease in means surface roughness as the gap voltage increases because this parameter initiates the discharge speed, which increases the stability and therefore decreases the surface roughness. The means and S/N ratio for material removal rate are shown in Figures 4.27 and 4.28.

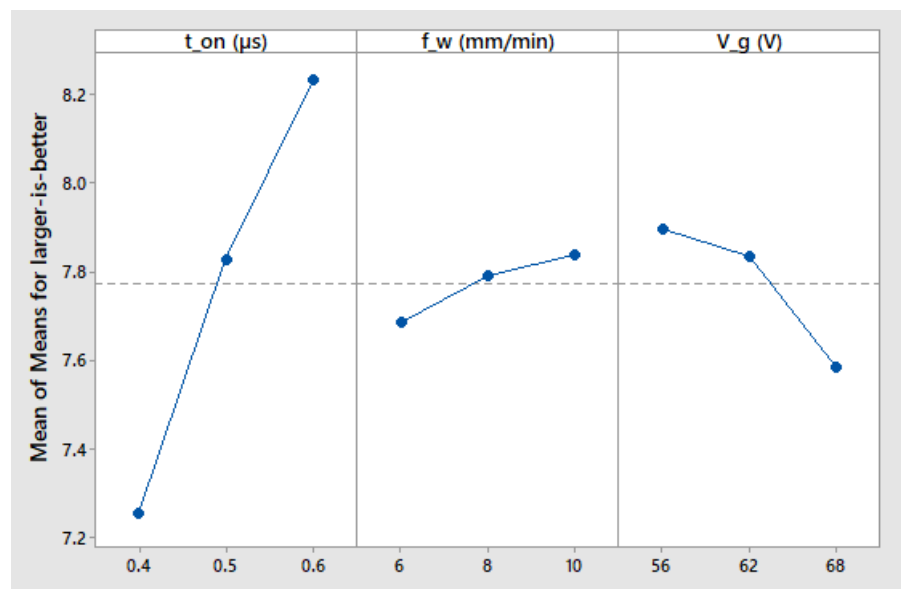


Figure 4.27: Main effects plot for Means of MRR

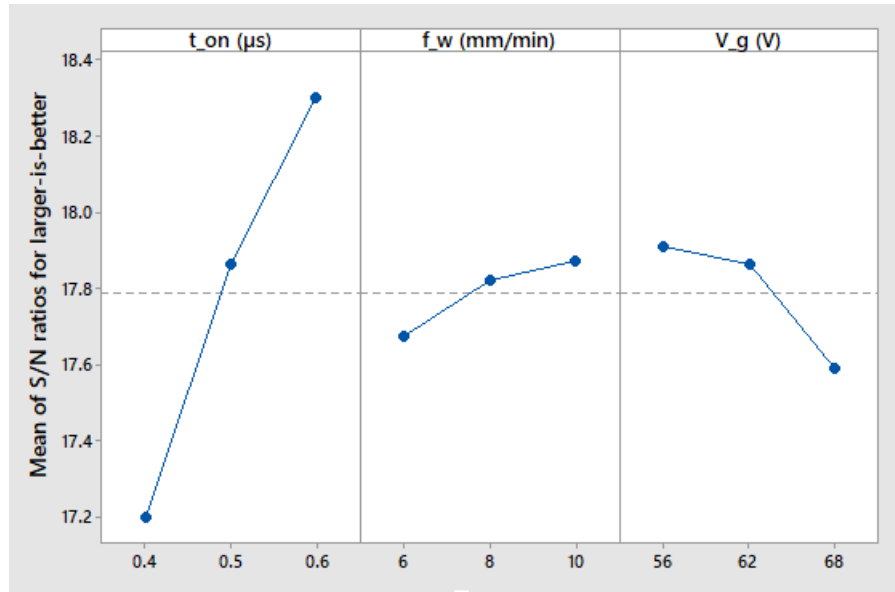


Figure 4.28: Main effects plot for S/N ratios of MRR

Figures 4.27 and 4.28 show the main effects plots for means and S/N ratio material removal rate. It can be seen that the means and S/N ratio for material removal rate were maximized for the pulse-on time, wire feed rate and gap voltage of $0.6 \mu\text{s}$, 10 mm/min and 56 V, respectively. The material removal rate increases with the increase in pulse-on time because of the higher peak discharge current produced as the pulse-on time to increases. It is also shown that the material removal rate decreases with the increase in gap voltage because the smaller value of gap voltage causes faster discharge speed. The material removal rate increases with the increase in wire feed rate because of more discharges produced as the wire feed rate increases.

In Minitab-17 $\text{\textcircled{R}}$, the nominal is best S/N ratio is used to find the optimal conditions for responses that are varying proportionally. The condition between the lowest level and the highest level is considered as optimal condition for both responses. It can be seen from Figures 4.25 and 4.27, that both material removal rate and surface roughness

vary proportionally with respect to pulse-on time, wire feed rate and gap voltage. Therefore, the nominal is best S/N ratio was applied for ANOVA and the generated main effects plots for mean and S/N ratio surface roughness and material removal rate are shown in Figures 4.29 and 4.30.

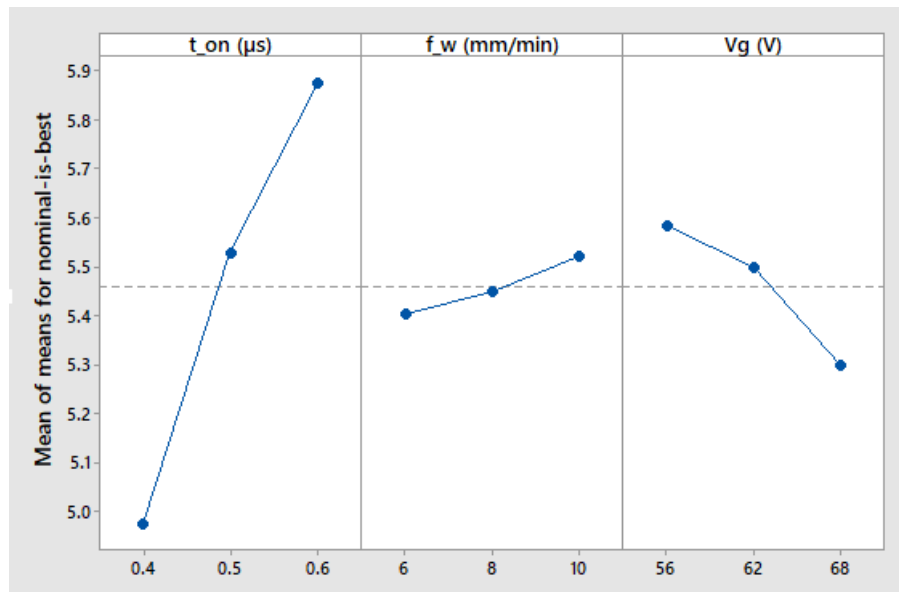


Figure 4.29: Main effects plot for means of SR and MRR

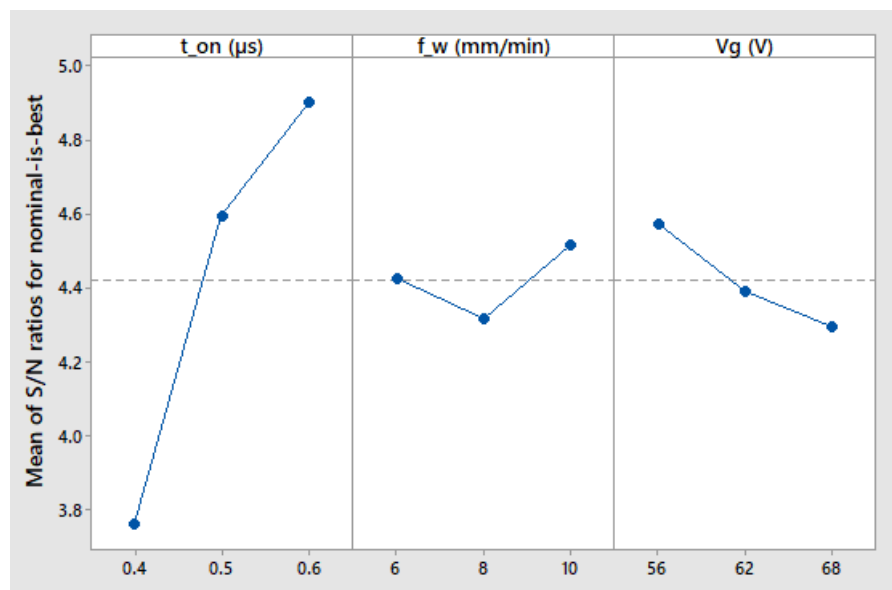


Figure 4.30: Main effects plot S/N ratio of SR and MRR

Figures 4.29 and 4.30 show the main effect plot for mean and S/N ratio for both surface roughness and material removal rate. In this case, it can be seen that the optimum conditions for both surface roughness and material removal rate are 0.5 μ s, 8 mm/min, 62 V for pulse-on time, wire feed rate and gap voltage respectively.

4.8 Validation of Optimal Control Parameters

Experimental work was done to validate the optimization process by setting control parameters to their corresponding optimum levels as obtained from optimization. Optimized and unoptimized surface roughness and material removal rate are shown in Figure is shown in Table 4.31.

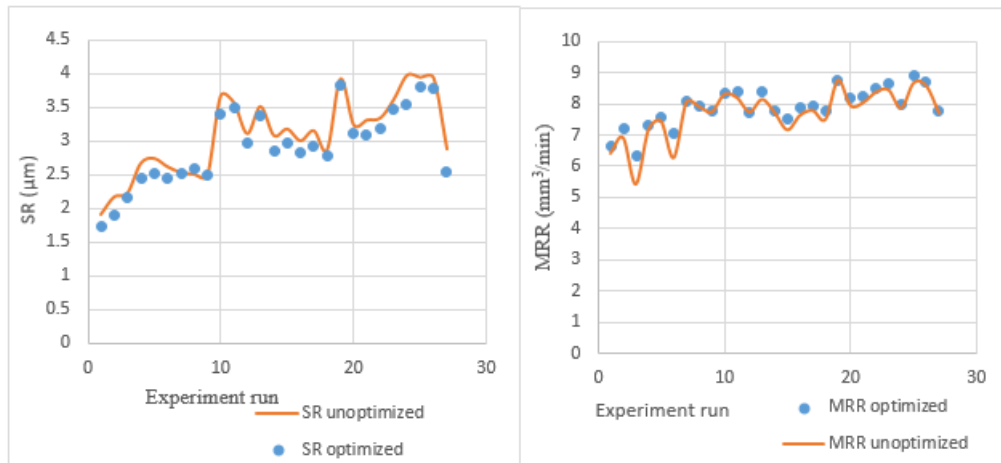


Figure 4.31: Optimized and unoptimized surface roughness

From Table 4.31, it can be seen that the value of surface roughness after optimization is lower than that of before. Also, the value of material removal rate after optimization is higher than before. This shows that there is an improvement resulted from optimization process.

4.9 Summary

As presented in this chapter, the most influential parameters are pulse-on time followed by wire feed rate and gap voltage for surface roughness, and pulse-on time followed by gap voltage and wire feed rate for material removal rate. From the model that was developed, an algorithm from which the graphical user interface displays predicted optimal machining conditions for each level of surface roughness or material removal rate required, is shown. From optimization, optimal conditions for each parameter, that give the best output are indicated. Finally, validation shows that there was an improvement by 5.68 % and 3.041 % for surface roughness and material removal rate, respectively.

CHAPTER FIVE

CONCLUSIONS AND RECOMMENDATIONS

5.1 Introduction

This section highlights briefly on conclusions made out of results obtained and recommendations suggested for further investigations.

In this work, investigation was performed on the influence of wire feed rate, gap voltage and pulse-on time on surface roughness and material removal rate in wire EDM of Inconel-625. Furthermore, mathematical model was developed to correlate input process parameters with output performance measures, of which an algorithm was developed to predict optimal machining parameter-levels. Finally, Taguchi technique was applied for optimization of the process for improved material removal rate and surface roughness.

From experimental investigations, it was confirmed that the pulse-on time, wire feed rate, and gap voltage are significant to the process. For surface roughness, pulse-on time is found to be the most influential parameter followed wire feed rate and gap voltage, while for material removal rate, pulse-on time is the most influential parameter followed by gap voltage and wire feed rate.

From optimization process, it was observed that the minimum surface roughness is achieved when pulse-on time, wire feed rate and gap voltage are set to $0.4 \mu s$, 8 mm/min and 68 V , respectively. The maximum material removal rate can be achieved when

these parameters, in the same order, are 0.6 μs , 10 mm/min, and 56 V, respectively, whereas for optimum surface roughness and material removal rate, these parameters could be, respectively, 0.5 μs , 8 mm/min, and 62 V. The optimization improved surface roughness and material removal rate by 5.68 % and 3.041 %, respectively.

The results from optimization will be applicable for machining of wire electrical discharge machining of Inconel-625 using brass wire as cutting wire and de-ionized water as dielectric fluid, regardless of the type of the wire EDM machine.

It is recommended that the investigation be extended to cover other performance parameters such as kerf width, corner accuracy and dielectric fluid flow rate.

5.2 Summary

This chapter presents the main findings of the work, and recommends accordingly. As the main contribution of this research to the body of knowledge, the minimum surface roughness and maximum material removal rate were improved since the most influential parameters on these responses were combined for optimization. Finally, with the algorithm developed, optimal machining conditions are obtained with minimum experimentation, thus reduces cost of production.

References

- Abbas, N. M., & Solomon, D. G. (2013). Electrical discharge machining (edm): Selection of dielectric in machining assab 718hh. In *Advanced materials research* (Vol. 622, pp. 520–524).
- Abbas, N. M., Solomon, D. G., & Bahari, M. F. (2007). A review on current research trends in electrical discharge machining (edm). *International Journal of machine tools and Manufacture*, 47(7-8), 1214–1228.
- Abhishek, K., Datta, S., Biswal, B. B., Mahapatra, S. S., et al. (2017). Machining performance optimization for electro-discharge machining of inconel 601, 625, 718 and 825: an integrated optimization route combining satisfaction function, fuzzy inference system and taguchi approach. *Journal of the Brazilian Society of Mechanical Sciences and Engineering*, 39(9), 3499–3527.
- Alexandrov, N. M., & Lewis, R. M. (2001). An overview of first-order model management for engineering optimization. *Optimization and Engineering*, 2(4), 413–430.
- Ali, M., Ammar, S., Baayah, N., Aishah, S., Zaliha, S., & Hayati, N. (n.d.). Optimization of edm parameters for micro/meso fabrication.
- Alias, A., Abdullah, B., & Abbas, N. M. (2012). Influence of machine feed rate in wedm of titanium ti-6al-4 v with constant current (6a) using brass wire. *Procedia Engineering*, 41, 1806–1811.
- Amorim, F., & Weingaertner, W. (2002). Influence of duty factor on the die-sinking

- electrical discharge machining of high-strength aluminum alloy under rough machining. *Journal of the Brazilian Society of Mechanical Sciences*, 24(3), 194–199.
- Ansari, S., & Bansal, A. (2017). *Investigation of edm machining parameters for inconel-625*. Unpublished doctoral dissertation, Lovely Professional University.
- Arminian, A., Kang, M., Kozak, M., Houshmand, S., & Mathews, P. (2008). Multipath: A comprehensive minitab program for computing path coefficients and multiple regression for multivariate analyses. *Journal of Crop Improvement*, 22(1), 82–120.
- Asgar, M. E., & Singholi, A. K. S. (2018). Parameter study and optimization of wedm process: A review. In *Iop conference series: Materials science and engineering* (Vol. 404, p. 012007).
- Babu, T. V., & Soni, J. (2017). Optimization of process parameters for surface roughness of inconel 625 in wire edm by using taguchi and anova method. *Int. J. Curr. Eng. Technol*, 7(3), 1127–1131.
- Banker, K., Parmar, S., & Parekh, B. (2013). Review to performance improvement of die sinking edm using powder mixed dielectric fluid. *Int. J. Res. Modern Eng. Emerg. Technol*, 1, 57–62.
- Baş, D., & Boyacı, I. H. (2007). Modeling and optimization i: Usability of response surface methodology. *Journal of food engineering*, 78(3), 836–845.
- Bezerra, M. A., Santelli, R. E., Oliveira, E. P., Villar, L. S., & Escaleira, L. A. (2008). Response surface methodology (rsm) as a tool for optimization in analytical chemistry. *Talanta*, 76(5), 965–977.
- Bisaria, H., & Shandilya, P. (2015). Machining of metal matrix composites by edm

- and it's variants: A review. *DAAAM International Scientific Book*.
- Bower, K. M. (2000). Analysis of variance (anova) using minitab. *Scientific Computing & Instrumentation*, 17, 64–65.
- Carley, K. M., Kamneva, N. Y., & Reminga, J. (2004). Response surface methodology: Casos technical report. *Center for Computational Analysis of Social and Organizational Systems, Carnegie Mellon University*.
- Carrano, A. L., Mehta, B., & Low, J. C. (2004). Response surface methodology of die-sink electro-discharge machined surfaces. In *Iie annual conference. proceedings* (p. 1).
- Chen, T. X., & Wang, C. Y. (2012). Investigation into roughness of surface polished by abrasive waterjet with taguchi method and dimensional analysis. In *Materials science forum* (Vol. 723, pp. 188–195).
- Chow, H., Yan, B., & Huang, F. (1999). Micro slit machining using electro-discharge machining with a modified rotary disk electrode (rde). *Journal of Materials Processing Technology*, 91(1-3), 161–166.
- Cramer, D. (2002). *Basic statistics for social research: Step-by-step calculations & computer techniques using minitab*. Routledge.
- Crookall, J., & Heuvelman, C. (1971). Electro-discharge machining the state of the art. *Annals of the CIRP*, 20(1), 113–120.
- Datta, S., Biswal, B. B., Mahapatra, S. S., et al. (2019). Machinability analysis of inconel 601, 625, 718 and 825 during electro-discharge machining: On evaluation of optimal parameters setting. *Measurement*, 137, 382–400.
- Deel, O. (1971). *Mechanical-property data inconel 625. annealed sheet* (Tech. Rep.).

BATTELLE COLUMBUS DIV OH.

- Devarasiddappa, D., George, J., Chandrasekaran, M., & Teyi, N. (2016). Application of artificial intelligence approach in modeling surface quality of aerospace alloys in wedm process. *Procedia Technology*, 25, 1199–1208.
- Dewangan, S. K. (2010). Experimental investigation of machining parameters for edm using u-shaped electrode of aisi p20 tool steel. *Department of Mechanical Engineering, National Institute of Technology Rourkela (India)*.
- Ghodsiyeh, D., Davoudinejad, A., Hashemzadeh, M., Hosseiniyehzad, N., & Golshan, A. (2013). Optimizing finishing process in wedming of titanium alloy (ti6al4v) by brass wire based on response surface methodology. *Research Journal of Applied Science, Engineering and Technology*, 5(4), 1290–1301.
- Giridharan, A., & Samuel, G. (2016). Analysis on the effect of discharge energy on machining characteristics of wire electrical discharge turning process. *Proceedings of the Institution of Mechanical Engineers, Part B: Journal of Engineering Manufacture*, 230(11), 2064–2081.
- Griffith, D. A. (1989). Spatial regression analysis on the pc: spatial statistics using minitab.
- Helsel, D. R. (2011). *Statistics for censored environmental data using minitab and r* (Vol. 77). John Wiley & Sons.
- Hewidy, M., El-Taweel, T., & El-Safty, M. (2005). Modelling the machining parameters of wire electrical discharge machining of inconel 601 using rsm. *Journal of Materials Processing Technology*, 169(2), 328–336.
- Jensen, W. A. (2008). *Doe simplified: Practical tools for effective experimentation*.

Journal of Quality Technology, 40(1), 124.

Jeong, I.-J., & Kim, K.-J. (2009). An interactive desirability function method to multiresponse optimization. *European Journal of Operational Research*, 195(2), 412–426.

Joshi, S., Sherali, H. D., & Tew, J. D. (1998). An enhanced response surface methodology (rsm) algorithm using gradient deflection and second-order search strategies. *Computers & operations research*, 25(7-8), 531–541.

Kansal, H., Singh, S., & Kumar, P. (2005). Parametric optimization of powder mixed electrical discharge machining by response surface methodology. *Journal of materials processing technology*, 169(3), 427–436.

Kansal, H., Singh, S., & Kumar, P. (2007). Effect of silicon powder mixed edm on machining rate of aisi d2 die steel. *Journal of Manufacturing processes*, 9(1), 13–22.

Karsh, P. K., & Singh, H. (2018). Multi-characteristic optimization in wire electrical discharge machining of inconel-625 by using taguchi-grey relational analysis (gra) approach: Optimization of an existing component/product for better quality at a lower cost. In *Design and optimization of mechanical engineering products* (pp. 281–303). IGI Global.

Krook, M., Recina, V., & Karlsson, B. (2005). Material properties affecting the machinability of inconel 718. In *Proceedings of the 6th international special emphasis symposium superalloys* (Vol. 718, pp. 625–706).

Kumar, K., Sivasubramanian, R., & Kalaiselvan, K. (2009). Selection of optimum parameters in non conventional machining of metal matrix composite. *Portugaliae*

Electrochimica Acta, 27(4), 477–486.

Kumar, K. G., Ramkumar, K. D., & Arivazhagan, N. (2015). Characterization of metallurgical and mechanical properties on the multi-pass welding of inconel 625 and aisi 316l. *Journal of Mechanical Science and Technology*, 29(3), 1039–1047.

Kumar, M., & Singh, H. (2018). Experimental investigation on surface integrity in machining of inconel x750 with wedm using taguchi technique. *International Journal of Process Management and Benchmarking*, 8(4), 516–530.

Lee, S., & Li, X. (2001). Study of the effect of machining parameters on the machining characteristics in electrical discharge machining of tungsten carbide. *Journal of materials processing Technology*, 115(3), 344–358.

Maher, I., Sarhan, A. A., & Hamdi, M. (2015). Review of improvements in wire electrode properties for longer working time and utilization in wire edm machining. *The International Journal of Advanced Manufacturing Technology*, 76(1-4), 329–351.

Mäkelä, M. (2017). Experimental design and response surface methodology in energy applications: a tutorial review. *Energy Conversion and Management*, 151, 630–640.

Mohan, B., Rajadurai, A., & Satyanarayana, K. (2004). Electric discharge machining of al–sic metal matrix composites using rotary tube electrode. *Journal of materials processing technology*, 153, 978–985.

Muthuramalingam, T., & Mohan, B. (2015). A review on influence of electrical process parameters in edm process. *Archives of civil and mechanical engineering*, 15(1), 87–94.

- Nelson, L. S. (1983). Exact critical values for use with the analysis of means. *Journal of Quality Technology*, 15(1), 40–44.
- Němeček, S., Fiedler, L., & Fišerová, P. (2015). Corrosion resistance of inconel 625 and austenitic steel m41 after laser claddings. In *Key engineering materials* (Vol. 647, pp. 115–120).
- Newton, T. R., Melkote, S. N., Watkins, T. R., Trejo, R. M., & Reister, L. (2009). Investigation of the effect of process parameters on the formation and characteristics of recast layer in wire-edm of inconel 718. *Materials Science and Engineering: A*, 513, 208–215.
- Nourbakhsh, F., Rajurkar, K. P., Malshe, A. P., & Cao, J. (2013). Wire electro-discharge machining of titanium alloy. *Procedia Cirp*, 5, 13–18.
- Pham, D. T., Dimov, S. S., Bigot, S., Ivanov, A., & Popov, K. (2004). Micro-edm recent developments and research issues. *Journal of materials processing technology*, 149(1-3), 50–57.
- Popa, M., Contiu, G., & Pop, G. (1866). Surface quality of the edm processed materials. In *Xix imeko world congress* (pp. 6–11).
- Prakash, C. (2008). A study on the machining characteristic in wire edm process. *Department of Mechanical Engineering, National Institute of Technology Rourkela (India)*.
- Pramanik, A., & Basak, A. (2019). Effect of wire electric discharge machining (edm) parameters on fatigue life of ti-6al-4v alloy. *International journal of fatigue*, 128, 105186.
- Rajmohan, T., Prabhu, R., Rao, G. S., & Palanikumar, K. (2012). Optimization of

- machining parameters in electrical discharge machining (edm) of 304 stainless steel. *Procedia engineering*, 38, 1030–1036.
- Rajurkar, K. P., Zhu, D., McGeough, J., Kozak, J., & De Silva, A. (1999). New developments in electro-chemical machining. *CIRP annals*, 48(2), 567–579.
- Rajyalakshmi, G., & Ramaiah, P. V. (2013). Optimization of process parameters of wire electrical discharge machining using fuzzy logic integrated with taguchi method. *International Journal of scientific engineering and technology*, 2(6), 594–600.
- Rao, G. K. M., Satyanarayana, S., & Praveen, M. (2008). Influence of machining parameters on electric discharge machining of maraging steels—an experimental investigation. In *Proceedings of the world congress on engineering* (Vol. 2, pp. 2–4).
- Rice, W. R. (1989). Analyzing tables of statistical tests. *Evolution*, 43(1), 223–225.
- Roy, R. K. (2001). *Design of experiments using the taguchi approach: 16 steps to product and process improvement*. John Wiley & Sons.
- Saha, S. K., & Choudhury, S. (2009). Experimental investigation and empirical modeling of the dry electric discharge machining process. *International Journal of Machine Tools and Manufacture*, 49(3-4), 297–308.
- Sahu, S. N. (2012). *Neural network modelling and multi-objective optimization of edm process* (Vol. 10). Unpublished doctoral dissertation.
- Sanders, J., Sarh, B., & Gökalp, I. (1997). Variable density effects in axisymmetric isothermal turbulent jets: a comparison between a first-and a second-order turbulence model. *International journal of heat and mass transfer*, 40(4), 823–842.

- Sanghani, C., & Acharya, G. (2016). A review of research on improvement and optimization of performance measures for electrical discharge machining.
- Sethy, R. (2014). *Experimental investigation and optimisation in edm process of aisi p20 tool steel*. Unpublished doctoral dissertation.
- Shah, C., Mevada, J., & Khatri, B. (2013). Optimization of process parameter of wire electrical discharge machine by response surface methodology on inconel-600. *International Journal of Emerging Technology and Advanced Engineering*, 3(4), 260–267.
- Sharma, P., Chakradhar, D., & Narendranath, S. (2015). Evaluation of wedm performance characteristics of inconel 706 for turbine disk application. *Materials & Design*, 88, 558–566.
- Singh, V. K., & Singh, S. (2015). Multi-objective optimization using taguchi based grey relational analysis for wire edm of inconel 625. *J. Mater. Sci. Mech. Eng*, 2(11), 38–42.
- Thidé, B. (2004). *Electromagnetic field theory*. Upsilon Books Uppsala, Sweden.
- Tonday, H., & Tigga, A. (2016). Analysis of effects of cutting parameters of wire electrical discharge machining on material removal rate and surface integrity. In *Iop conference series: Materials science and engineering* (Vol. 115, p. 012013).
- Va, M. K., Ab, S. B., Rc, V., & Md, R. (2010). Optimization of the wedm parameters on machining incoloy800 super alloy with multiple quality characteristics. *Optimization*, 2(6), 1538–1547.
- Vates, U., Singh, N. K., & Singh, R. (2016). Modelling and optimisation of wire electrical discharge machining process on d2 steel using ann and rmse approach.

International Journal of Computational Materials Science and Surface Engineering, 6(3-4), 161–185.

Velleman, P. F., & Welsch, R. E. (1981). Efficient computing of regression diagnostics. *The American Statistician*, 35(4), 234–242.

Wang, D., & Conerly, M. (2003). Evaluation of three lack of fit tests in linear regression models. *Journal of Applied Statistics*, 30(6), 683–696.

Yamazaki, K. (1998, May 26). *Method of surface roughness measurement using a fiber-optic probe*. Google Patents. (US Patent 5,757,496)

Yangfan, W., Xizhang, C., & Chuanchu, S. (2019). Microstructure and mechanical properties of inconel 625 fabricated by wire-arc additive manufacturing. *Surface and Coatings Technology*, 374, 116–123.

APPENDICES

Appendix I: Composition of the Specimen Used

Table A.1: Composition of chemicals in Inconel-625

Element	Percentage (%)
Nickel	58
Chromium	20
Iron	5
Molybdenum	8
Niobium	4.15
Carbon	0.1
Manganese	0.5
Silicon	0.5
Phosphorus	0.015
Sulfur	0.015
Aluminum	0.4
Titanium	0.4
Cobalt	1
Total=100%	

Appendix II: Surface Roughness Measurement

When using Mitutoyo-SJ-30 to measure surface roughness, it is required to refer to some standards such as the *JSB0601-2001 and ISO* standard. For example, when the value of R_a falls between $2 \mu m$ and $10 \mu m$, the sampling and evaluation lengths should be set to 2.5 and 12.5 mm respectively.

Table B.1: JSB0601-2001 and ISO standard for surface roughness measurement

Range of $R_a(\mu m)$	Sampling length (mm)	Evaluation length (mm)
$0.006 < R_a < 0.02$	0.08	0.4
$0.02 < R_a < 0.1$	0.25	1.25
$0.1 < R_a < 2$	0.8	4
$2 < R_a < 10$	2.5	12.5
$10 < R_a < 80$	8	40

Appendix III: Effect of Input Process Parameters on Machining Output

Table C.1: Preliminary results on the effect of pulse-on time on surface roughness and material removal rate

Run	t_{on} (μs)	SR (μm)	MRR (mm^3/min)
1	0.4	2.9312	3.7998
2	0.45	2.9511	3.8807
3	0.5	2.9101	3.8975
4	0.55	2.9512	3.8926
5	0.6	2.9822	3.8818
6	0.65	3.1531	4.5886
7	0.7	3.3211	4.5477
8	0.75	3.0712	4.2725
9	0.8	3.4523	4.7939
10	0.85	3.6811	5.1720
11	0.9	3.6731	5.1997
12	0.95	3.4911	5.0936
13	1	3.6912	5.9947
14	1.05	3.7811	6.3881
15	1.1	3.7422	6.2852
16	1.15	3.7211	6.1515
17	1.2	3.8112	6.7305

Table C.2: Preliminary results on the effect of gap voltage on surface roughness and material removal rate

Run	v_g (V)	SR (μm)	MRR	Run	v_g (V)	SR (μm)	MRR
1	20	3.9511	6.7305	23	86	2.8921	4.2725
2	22	3.9421	6.5262	24	89	2.9722	4.3412
3	25	3.9112	6.388	25	92	2.9812	4.4329
4	28	3.9221	6.3523	26	95	2.8912	3.9618
5	31	3.8712	6.2858	27	98	2.8543	3.9989
6	34	3.8321	6.3447	28	100	2.8122	3.9452
7	37	3.7912	6.1515	29	101	2.87215	4.102
8	40	3.7512	6.0555	30	104	2.8912	3.7726
9	43	3.7112	5.9947	31	107	2.8111	3.9127
10	47	3.4532	6.0037	32	109	2.7218	3.8691
11	50	3.3132	5.172	33	113	2.8221	3.9968
12	53	3.1612	5.3123	34	116	2.7129	3.7635
13	56	3.0521	5.0997	35	122	2.7127	3.8459
14	59	3.0421	5.1368	36	125	2.7127	3.8387
15	62	3.0332	5.1353	37	128	2.7128	3.9807
16	65	3.0312	5.1352	38	131	2.7316	3.8336
17	68	3.0357	5.1299	39	134	2.7126	3.7759
18	71	2.9312	4.7921	40	137	2.7314	3.7298
19	74	2.9522	4.5881	41	140	2.7135	3.4118
20	77	2.9112	4.6355	42	143	2.7135	3.4447
21	80	2.9422	4.5477	43	146	2.7134	3.6407
22	83	2.9312	4.6176	44	150	2.7312	3.4894

Table C.3: Preliminary results on the effect of wire feed rate on surface roughness and material removal rate

Run	f_w (mm/min)	SR (μm)	MRR (mm^3/min)
1	1	2.4911	3.64079
2	2	2.5221	3.86971
3	3	2.5512	3.88215
4	4	2.5912	3.93639
5	5	2.6913	4.12577
6	6	2.7931	4.40673
7	7	2.6412	4.49034
8	8	2.4931	4.65599
9	9	2.5412	4.61028
10	10	2.5612	4.61996
11	11	2.9323	5.0625
12	12	3.1523	5.31234
13	13	3.2421	5.89658
14	14	3.3912	6.15381
15	15	3.4511	6.16712

Table C.4: Effect of pulse-on time, gap voltage and wire feed rate on surface roughness and material removal rate

Run	t_{on} (μs)	f_w (mm/min)	V_g (V)	SR (μm)	MRR (mm^3/min)
1	0.4	6	56	1.9162	6.4061
2	0.4	6	62	2.1752	6.9021
3	0.4	6	68	2.2322	5.4189
4	0.4	8	56	2.6732	7.1571
5	0.4	8	62	2.7472	7.4342
6	0.4	8	68	2.6243	6.2642
7	0.4	10	56	2.540	8.0288
8	0.4	10	62	2.512	7.9012
9	0.4	10	68	2.4903	7.7212
10	0.5	6	56	3.6745	8.2844
11	0.5	6	62	3.5735	8.1834
12	0.5	6	68	3.1132	7.7231
13	0.5	8	56	3.5172	8.1271
14	0.5	8	62	3.0862	7.6961
15	0.5	8	68	3.1832	7.1531
16	0.5	10	56	3.0093	7.6192

Table C.5: Effect of pulse-on time, gap voltage and wire feed rate on surface roughness and material removal rate (Continued)

Run	t_{on} (μs)	f_w	V_g (V)	SR (μm)	MRR (mm^3/min)
17	0.5	10	62	3.1582	7.7681
18	0.5	10	68	2.8744	7.4843
19	0.6	6	56	3.9243	8.7342
20	0.6	6	62	3.243	7.9242
21	0.6	6	68	3.3153	8.0252
22	0.6	8	56	3.3463	8.3564
23	0.6	8	62	3.6195	8.4294
24	0.6	8	68	3.9792	7.8431
25	0.6	10	56	3.9481	8.6580
26	0.6	10	62	3.9392	8.5491
27	0.6	10	68	2.8872	7.6871

Appendix IV: Predicted and Experimental Output Readings

Table D.1: The experimental and predicted values for surface roughness and material removal rate

Run	t_{on} (μs)	f_w	V_g (V)	SR (μm)		MRR (mm^3/min)	
				Pred	Exp	Pred	Exp
1	0.4	6	56	1.7294	1.9162	6.6498	6.4061
2	0.4	6	62	1.9100	2.1752	7.2122	6.9021
3	0.4	6	68	2.1546	2.2322	6.3456	5.4189
4	0.4	8	56	2.4556	2.6732	7.3059	7.1571
5	0.4	8	62	2.5157	2.7472	7.5670	7.4342
6	0.4	8	68	2.4569	2.6243	7.030276	6.2642
7	0.4	10	56	2.5265	2.5401	8.0627	8.0288
8	0.4	10	62	2.5860	2.5120	7.9225	7.9012
9	0.4	10	68	2.4855	2.4903	7.7845	7.7212
10	0.5	6	56	3.4113	3.6745	8.3329	8.2844
11	0.5	6	62	3.4900	3.5735	8.3880	8.1834
12	0.5	6	68	2.9688	3.1132	7.74537	7.7231
13	0.5	8	56	3.3724	3.5172	8.3932	8.1271
14	0.5	8	62	2.8504	3.0862	7.7471	7.6961
15	0.5	8	68	2.9728	3.1832	7.50318	7.1531
16	0.5	10	56	2.8381	3.0093	7.8543	7.6192

Table D.2: Predicted and experimental values for surface roughness and material removal rate (continued)

Run	t_{on} (μs)	f_w	V_g (V)	SR (μm)		MRR (mm^3/min)	
				Pred	Exp	Pred	Exp
17	0.4	10	62	2.9155	3.1582	7.9069	7.7681
18	0.4	10	68	2.7931	2.8744	7.7517	7.4843
19	0.6	6	56	3.8404	3.9243	8.7504	8.7342
20	0.6	6	62	3.1171	3.243	8.1883	7.9242
21	0.6	6	68	3.0839	3.3153	8.2384	8.0252
22	0.6	8	56	3.1962	3.3463	8.5050	8.3564
23	0.6	8	62	3.4623	3.6195	8.6517	8.4294
24	0.6	8	68	3.5359	3.9792	8.0005	7.8431
25	0.6	10	56	3.7967	3.9481	8.9103	8.658
26	0.6	10	62	3.7722	3.9392	8.7158	8.5491
27	0.6	10	68	2.5477	2.8872	7.7633	7.6871

Appendix V: Analysis of Variance Parameters

1. Adjusted sum of squares

The model's various components can be represented as measures of variation as adjusted sums of squares (Adj SS). As per the ANOVA Table, the purpose of the Minitab is to separate the sum of squares into various different components. This helps variation description due to different sources. The order of the predictors in the model doesn't affect the Adj SS calculation. Calculation of a term's p-value is done by the Minitab using the adjusted sums of squares. P-values are interpreted instead of the sums of squares.

2. Degree of freedom

The total degrees of freedom (DF) help in estimation of the unknown population parameters. The number of observations in the sample helps in determining the total DF. Once the sample size is increased, more information about the population is provided resulting to an increased total DF. More information is required to increase the number of terms used in the model thus decreasing the DF available in estimation of the variability of the parameters. The DF is partitioned for error by the Minitab if the two conditions are met. Availability of terms to fit data not included in the model is the most significant condition.

3. F-value

The F-value appears for every term in the variance table analysis. The F-value is a test statistic that helps determine that the term used relates to the response. Using the Minitab, the p-value is calculated by the F-value. The p-value helps

in making decision on statistical importance of the terms of model.

4. P-value

The p-value refers to a probability used to measure the evidence against the null hypothesis. Stronger evidence is provided by the lower probabilities upon the null hypothesis.

5. Adjusted mean squares

Adjusted mean squares (Adj MS) helps to measure the variation that can be explained by a model or a term. It should be in assumption that all other terms are in the model without considering the order in which they were entered. The degrees of freedom are considered by the adjusted mean squares unlike the adjusted sums of squares . Minitab uses the adjusted mean squares to calculate the p-value for a term and the adjusted R^2 statistic.

Appendix VI: MATLAB Code for Graphical User Interface

```
function varargout = claverGUI4(varargin)

% CLAVERGUI4 MATLAB code for claverGUI4.fig

%     CLAVERGUI4, by itself, creates a new CLAVERGUI4 or raises the
%
%     existing
%
%     singleton*.
%
%     H = CLAVERGUI4 returns the handle to a new CLAVERGUI4 or the
%
%     handle to
%
%     the existing singleton*.
%
%
%     CLAVERGUI4('CALLBACK',hObject,eventData,handles,...) calls the
%
%     local
%
%     function named CALLBACK in CLAVERGUI4.M with the given input
%
%     arguments.
%
%
%     CLAVERGUI4('Property','Value',...) creates a new CLAVERGUI4 or
%
%     raises the
%
%     existing singleton*. Starting from the left, property value
%
%     pairs are
%
%     applied to the GUI before claverGUI4_OpeningFcn gets called.
%
%     An
%
%     unrecognized property name or invalid value makes property
%
%     application
```

```

%      stop. All inputs are passed to claverGUI4_OpeningFcn via
varargin.

%

%      *See GUI Options on GUIDE's Tools menu. Choose "GUI allows
only one

%      instance to run (singleton)".

%

% See also: GUIDE, GUIDATA, GUIHANDLES

% Edit the above text to modify the response to help claverGUI4

% Last Modified by GUIDE v2.5 29-Oct-2019 23:41:29

% Begin initialization code - DO NOT EDIT

gui_Singleton = 1;

gui_State = struct('gui_Name',      mfilename, ...
'gui_Singleton',  gui_Singleton, ...
'gui_OpeningFcn', @claverGUI4_OpeningFcn, ...
'gui_OutputFcn',  @claverGUI4_OutputFcn, ...
'gui_LayoutFcn',  [] , ...
'gui_Callback',   []);

if nargin && ischar(varargin{1})

gui_State.gui_Callback = str2func(varargin{1});

```

```

end

if nargin
[varargout{1:nargout}] = gui_mainfcn(gui_State, varargin{:});
else
gui_mainfcn(gui_State, varargin{:});
end

% End initialization code - DO NOT EDIT

% --- Executes just before claverGUI4 is made visible.

function claverGUI4_OpeningFcn(hObject, eventdata, handles, varargin)

% This function has no output args, see OutputFcn.

% hObject    handle to figure

% eventdata  reserved - to be defined in a future version of MATLAB

% handles    structure with handles and user data (see GUIDATA)

% varargin   command line arguments to claverGUI4 (see VARARGIN)

% Choose default command line output for claverGUI4

handles.output = hObject;

% Update handles structure

guidata(hObject, handles);

% UIWAIT makes claverGUI4 wait for user response (see UIRESUME)

% uiwait(handles.figure1);

% --- Outputs from this function are returned to the command line.

function varargout =

claverGUI4_OutputFcn(hObject, eventdata, handles)

```

```

% varargout  cell array for returning output args (see VARARGOUT);
% hObject    handle to figure
% eventdata  reserved - to be defined in a future version of MATLAB
% handles    structure with handles and user data (see GUIDATA)
% Get default command line output from handles structure
varargout{1} = handles.output;

% --- Executes on button press in pushbutton1.

function pushbutton1_Callback(hObject, eventdata, handles)

% hObject    handle to pushbutton1 (see GCBO)
% eventdata  reserved - to be defined in a future version of MATLAB
% handles    structure with handles and user data (see GUIDATA)

syms TON1;syms TON2;f_w =(6+10+10)/4; v_g=(56+56+62)/3;

SR1=(0.795+1.535*TON1+0.0241*f_w-0.00108*v_g)^2==3;

TON1=vpa(solve(SR1,TON1));

TONN1=TON1(TON1>=0);

ton_min=sprintf('%.2f',TONN1);

SR2=(0.795+1.535*TON2+0.0241*f_w-0.00108*v_g)^2==4;

TON2=vpa(solve(SR2,TON2));

TONN2=TON2(TON2>=0);

ton_max=sprintf('%.2f',TONN2);

disp('Optimal parameters for a very rough surface');

T=table(ton_min,ton_max,v_g,f_w)

% --- Executes on button press in pushbutton2.

```



```

function pushbutton2_Callback(hObject, eventdata, handles)

% hObject    handle to pushbutton2 (see GCBO)
% eventdata  reserved - to be defined in a future version of MATLAB
% handles    structure with handles and user data (see GUIDATA)

syms TON1;syms TON2; f_w=(8+8+10+10+10+6+8+8+10+10+10+8+10)/13;

v_g=(62+68+56+62+68+68+62+68+56+62+68+68+68)/13;

SR1=(0.795+1.535*TON1+0.0241*f_w-0.00108*v_g)^2==2.5;

TON1=vpa(solve(SR1,TON1));

TONN1=TON1(TON1>=0);

ton_min=sprintf('%.2f',TONN1);

SR2=(0.795+1.535*TON2+0.0241*f_w-0.00108*v_g)^2==3;

TON2=vpa(solve(SR2,TON2));

TONN2=TON2(TON2>=0);

ton_max=sprintf('%.2f',TONN2);

disp('Optimal parameters for Rough surface');

T=table(ton_min,ton_max,v_g,f_w)

% --- Executes on button press in pushbutton3.

function pushbutton3_Callback(hObject, eventdata, handles)

% hObject    handle to pushbutton3 (see GCBO)
% eventdata  reserved - to be defined in a future version of MATLAB
% handles    structure with handles and user data (see GUIDATA)

syms TON1;syms TON2; f_w=(6+8)/2; v_g=(62+56)/2;

SR1=(0.795+1.535*TON1+0.0241*f_w-0.00108*v_g)^2==1;

```

```

TON1=vpa(solve(SR1,TON1));

TONN1=TON1(TON1>=0);

ton_min=sprintf('%.2f',TONN1);

SR2=(0.795+1.535*TON2+0.0241*f_w-0.00108*v_g)^2==2.5;

TON2=vpa(solve(SR2,TON2));

TONN2=TON2(TON2>=0);

ton_max=sprintf('%.2f',TONN2);

disp('Optimal parameters for a smooth surface');

T=table(ton_min,ton_max,v_g,f_w)

% --- Executes on button press in pushbutton4.

function pushbutton4_Callback(hObject, eventdata, handles)

% hObject    handle to pushbutton4 (see GCBO)
% eventdata  reserved - to be defined in a future version of MATLAB
% handles    structure with handles and user data (see GUIDATA)

syms TON1;syms TON2; f_w=(6+6+8+8+10+10+10+8+10+10)/10;

v_g=(62+68+62+68+56+62+68+68+62+68)/10;

MRR1=(1.932+1.106*TON1+0.00968*f_w-0.00543*v_g)^2==4.5;

TON1=vpa(solve(MRR1,TON1));

TONN1=TON1(TON1>=0);

ton_min=sprintf('%.2f',TONN1);

MRR2=(1.932+1.106*TON2+0.00968*f_w-0.00543*v_g)^2==6;

TON2=vpa(solve(MRR2,TON2));

```

```

TONN2=TON2(TON2>=0);

ton_max=sprintf('%.2f',TONN2);

disp('Optimal parameters for very fast cutting speed');

T=table(ton_min,ton_max,v_g,f_w)

% --- Executes on button press in pushbutton5.

function pushbutton5_Callback(hObject, eventdata, handles)

% hObject    handle to pushbutton5 (see GCBO)
% eventdata  reserved - to be defined in a future version of MATLAB
% handles    structure with handles and user data (see GUIDATA)

syms TON1;syms TON2; f_w=(8+10+10)/3; v_g=(68+56+62)/3;

MRR1=(1.932+1.106*TON1+0.00968*f_w-0.00543*v_g)^2==4;

TON1=vpa(solve(MRR1,TON1));

TONN1=TON1(TON1>=0);

ton_min=sprintf('%.2f',TONN1);

MRR2=(1.932+1.106*TON2+0.00968*f_w-0.00543*v_g)^2==4.5;

TON2=vpa(solve(MRR2,TON2));

TONN2=TON2(TON2>=0);

ton_max=sprintf('%.2f',TONN2);

disp('Optimal parameters for fast cutting speed');

T=table(ton_min,ton_max,v_g,f_w)

% --- Executes on button press in pushbutton6.

function pushbutton6_Callback(hObject, eventdata, handles)

% hObject    handle to pushbutton6 (see GCBO)

```

```

% eventdata reserved - to be defined in a future version of MATLAB

% handles structure with handles and user data (see GUIDATA)

syms TON1;syms TON2; f_w=10; v_g=68;

MRR1=(1.932+1.106*TON1+0.00968*f_w-0.00543*v_g)^2==3;

TON1=vpa(solve(MRR1,TON1));

TONN1=TON1(TON1>=0);

ton_min=sprintf('%.2f',TONN1);

MRR2=(1.932+1.106*TON2+0.00968*f_w-0.00543*v_g)^2==4;

TON2=vpa(solve(MRR2,TON2));

TONN2=TON2(TON2>=0);

ton_max=sprintf('%.2f',TONN2);

disp('Optimal parameters for slow cutting speed');

T=table(ton_min,ton_max,v_g,f_w)

```

Appendix VII: Publications

1. Claver Nsanzumuhire, Bernard W. Ikua and Karanja Kabini “Optimization of Wire Electrical Discharge Machining of Inconel-625”, International Journal of Engineering, Technology and Scientific Innovation, Vol 4, 2019.